

OPTIMIZING *IN PLANTA* TRANSFORMATION METHODS IN RICE (*ORYZA*
SATIVA) USING CARBON NANOTUBES

A Thesis by

TIA KEI DUNBAR

Submitted to the Graduate and Professional School of
Texas A&M University
in partial fulfillment of the requirements for the degree of

MASTER OF SCIENCE

Chair of Committee,	Michael J. Thomson
Co-Chair Member,	David M. Stelly
Committee Member,	Sakiko Okumoto

Head of Department,	David Baltensperger
---------------------	---------------------

December 2021

Major Subject: Plant Breeding

Copyright 2021 Tia K. Dunbar

ABSTRACT

CRISPR/Cas-based gene editing technologies offer the potential to precisely modify crops; however, *in vitro* plant transformation and regeneration techniques present a bottleneck due to the lengthy and genotype-specific tissue culture process. Ideally, *in planta* transformation can bypass tissue culture and directly lead to transformed plants, but efficient *in planta* delivery and transformation remains a challenge. Our research investigates transformation methods that have the potential to directly alter germline cells, eliminating the challenge of *in vitro* plant regeneration. Recent studies have demonstrated that carbon nanotubes (CNTs) loaded with plasmid DNA can diffuse through plant cell walls, facilitating transient expression of foreign genetic elements in plant tissues. Therefore, CNTs delivering CRISPR/Cas expressing vectors into mature embryos should be able to create heritable genetic edits. To test this hypothesis, CNT delivery into rice tissues was initially tested using leaf infiltration with reporter genes. After showing successful passive delivery of plasmid-carrying CNTs expressing reporter genes into leaves, rice seeds and excised mature embryos were then tested for CNT-based delivery of CRISPR/Cas reagents. The phytoene desaturase gene was targeted for knockout as homozygous or biallelic knockouts result in albino phenotypes. Rice seeds and excised embryos were imbibed in CRISPR plasmid-CNT solutions, and successful delivery and gene editing was observed visually and by sequencing. Data indicate that CNTs transporting CRISPR vectors are capable of passive diffusion and transient expression in rice tissues. Moreover, a similar approach was initiated in cotton pollen

tubes, but more work is needed to keep the pollen tubes from rupturing in the CNT solution. Overall, the results show that CNT-based delivery shows promise for *in planta* transformation and further optimization of our gene editing protocol has the potential to accelerate crop improvement to meet the challenges of future global crop production.

DEDICATION

I dedicate this to my Mom, who always encouraged me to do my best and who worked tirelessly to support me at every step of my journey. Thank you for inspiring my tenacious work ethic.

ACKNOWLEDGEMENTS

I would like to thank my committee chair, Dr. Michael Thomson, as well as Drs. David Stelly and Sakiko Okumoto, who also served on my committee. I truly appreciate their feedback and encouragement throughout my research.

A huge thanks goes out to the Texas A&M Institute for Genome Sciences and Society (TIGSS), Microscopy and Imaging Center (MIC), and AgriGenomics Lab (AGL) for providing me their services, equipment, and expertise. An additional thanks to the Landry Lab at UC Berkeley, especially to Dr. Gözde Demirer, for their crucial help surrounding carbon nanotubes.

Finally, I thank the members of the Texas A&M Crop Gene Editing Lab who offered invaluable guidance whenever I needed it. I truly could not have completed my research without the support of our lab's post-doc and fellow graduate students: Dr. Nikolaos Tsakirpaloglou, Sudip, Aya, Mason, Oneida, Serina, and Dr. Nancy Wahl.

CONTRIBUTORS AND FUNDING SOURCES

Contributors

This work was supervised by a thesis committee consisting of Drs. Michael Thomson and Sakiko Okumoto of the Department of Soil and Crop Sciences and Dr. David Stelly of the Interdisciplinary Graduate Program in Genetics.

All other work conducted for this thesis was completed by the student independently.

Funding Sources

Graduate study was supported by the Graduate Diversity Excellence Fellowship from Texas A&M University.

This work was also made possible in part by funding provided by Texas A&M AgriLife Research to the Crop Genome Editing Lab, by the Texas A&M University X-Grant project through the President's Excellence Fund (PI Michael J. Thomson), and by the USDA National Institute of Food and Agriculture under AFRI Grant Number 2020-67013-31811. Its contents are solely the responsibility of the authors and do not necessarily represent the official views of Texas A&M AgriLife Research or the USDA National Institute of Food and Agriculture.

NOMENCLATURE

cDNA	Complementary DNA
CNT	Carbon Nanotube
CRISPR	Clustered Regularly Interspaced Short Palindromic Repeats
GFP/YFP	Green/Yellow Fluorescent Protein
GUS	β -Glucuronidase
MES	2-(N-morpholino)-ethanesulfonic acid
PCR	Polymerase chain reaction
pDNA	Plasmid DNA
<i>PDS</i>	<i>PHYTOENE DESATURASE</i>
PEI	Polyethylenimine
RT-PCR	Reverse transcription PCR
SAM	Shoot Apical Meristem
sgRNA	Single-guide RNA
TAMU	Texas A&M University

TABLE OF CONTENTS

	Page
ABSTRACT	II
DEDICATION	IV
ACKNOWLEDGEMENTS	V
CONTRIBUTORS AND FUNDING SOURCES.....	VI
NOMENCLATURE.....	VII
TABLE OF CONTENTS	VIII
LIST OF FIGURES.....	X
LIST OF TABLES	XIII
1. INTRODUCTION.....	14
1.1. CRISPR Systems for Gene Editing.....	15
1.2. Current CRISPR Delivery Methods for Gene Editing in Plants	16
1.3. Gene Editing with Nanoparticles	17
1.4. Phytoene Desaturase	18
1.5. Pollen Tubes.....	18
1.6. Rationale and Objectives.....	19
2. TRANSIENT EXPRESSION OF REPORTER PLASMIDS IN RICE TISSUES BY CNT INFILTRATION.....	22
2.1. Synopsis	22
2.2. Introduction	22
2.3. Materials and Methods.....	23
2.3.1. pDNA-PEI-CNT Preparation	23
2.3.2. Transformation Vectors.....	24
2.3.3. Leaf Infiltrations with CNTs	24
2.3.4. CNT Infiltration of Rice Seeds with Reporter Plasmids	25
2.3.5. CNT Infiltration of Shoot Apical Meristems with Reporter Plasmids	26
2.3.6. Fluorescent Transcript Confirmation	26
2.3.7. Confocal Imaging of Nuclear-Localized GFP.....	27

2.3.8. GUSPlus Transcript Confirmation	27
2.4. Results	28
2.4.1. Transient Fluorescence in Rice Leaves and Embryos.....	28
2.5. Discussion	40
3. GENE EDITING BY TRANSIENT EXPRESSION OF CRISPR/CAS VECTORS BY CNT INFILTRATION.....	45
3.1. Synopsis	45
3.2. Introduction	45
3.3. Materials and Methods	46
3.3.1. Transformation Vectors.....	46
3.3.2. Transient Expression of CRISPR/Cas9 System Targeting <i>OsPDS</i>	47
3.3.3. Sanger Sequencing Screening for <i>OsPDS</i> Mutations.....	48
3.3.4. Confirming <i>OsPDS</i> Gene Editing by NGS	49
3.4. Results	49
3.4.1. Visual Analysis of Aberrant Phenotypes.....	49
3.4.2. DNA Sequencing of Potential Phenotypic Anomalies.....	51
3.5. Discussion	55
4. <i>IN VITRO</i> COTTON POLLEN TUBE GROWTH AND CNT INFILTRATION.....	59
4.1. Synopsis	59
4.2. Introduction	59
4.3. Materials and Methods	60
4.3.1. Cotton Pollen Tube Media Optimization	60
4.3.2. Infiltration of Pollen Tubes with CNTs.....	61
4.4. Results	61
4.5. Discussion	70
5. CONCLUSIONS	74
APPENDIX SUPPLEMENTAL FIGURES AND TABLES.....	83

LIST OF FIGURES

	Page
Figure 1. Rice leaf infiltration using binary and nonbinary plasmid vectors encoding GFP driven by CmYLCV promoters. CNT solution consists of a 2:1 pDNA:CNT ratio. Leftmost columns indicate exposure time.	29
Figure 2. Rice leaves three days post-infiltration with binary CmYLCV::GFP pDNA-CNT solutions at 2:1, 4:1, or 6:1 pDNA:CNT ratios. Leftmost columns indicate exposure time.	30
Figure 3 A. Excised rice embryos three days post-imbibe with CaMV 35S::GFP or ZmUbi::EYFP compared to plasmid-only and CNT-only controls. Solutions consist of 1:3 pDNA:CNT ratios. RNA was extracted and synthesized into cDNA, then amplified with GFP- or EYFP-specific primers following HF Phusion polymerase parameters. B. Products were run on a 1.5% agarose gel for 75 minutes at 50V. Ladder: GeneRuler 1kb Plus.....	33
Figure 4. Average corrected total fluorescence of rice leaves over a period of ten days. Corrected total fluorescence was determined by subtracting the mean fluorescent noise from each sample reading from ImageJ. Asterisks indicate significantly different fluorescence determined by Tukey's HSD.	34
Figure 5. Excised embryos infiltrated with CNTs and NLS-GFP reporter plasmids were imaged under Olympus SZX10 and Echo Revolve stereomicroscopes after three days post-imbibe.....	35
Figure 6. Excised leaves and embryos treated with CNTs carrying NLS-GFP vectors were sectioned, stained with DRAQ5, and imaged under confocal microscope after four days in solution. A, B, and C seem to indicate GFP fluorescence overlap with nuclear staining, but high levels of noise in negative controls (D) and unlocalized fluorescence in other treated samples (E) prevent us from drawing definitive conclusions. Sectioning and imaging performed by TAMU MIC.	36
Figure 7. Rice leaves were punctured with needles and imbibed in CNTs loaded with GUSPlus vectors. After three days in solution, GUSPlus enzymatic activity was visualized by histochemical assay (Cervera, 2004) and chlorophyll bleaching. Blue coloration indicates GUSPlus activity in treated leaves at the infiltration site.....	38
Figure 8. Oligo(dT) primers were used to synthesize cDNA from RNA extracted from GUSPlus-CNT treated rice leaves. A. Housekeeping primers specific to EFA were used to PCR amplify cDNA. Bands around 200 bp are indicative	

of successful cDNA synthesis from processed mRNA. B. Primers specific to GUSPlus were used to amplify a 160 bp fragment in the presence of GUSPlus transcripts C. Primers targeting the hygromycin resistance gene of the GUSPlus plasmid backbone amplified a 360 bp fragment only in the presence of residual pDNA.....	39
Figure 9. <i>OsPDS</i> sgRNAs were designed to target the third and fourth exons of both Nipponbare and Presidio genotypes. Target sequences are outlined in red, and the PAM is underlined.	47
Figure 10. Subset of seeds that were imbibed in pDNA-CNT solutions in 2:1, 1:1, and 1:2 ratios of CRISPR/Cas vectors to CNTs. Seeds were grown on MS0 media plates for up to two weeks. Experimental seeds (A-C) that showed altered growth compared to control seeds (D, E) were used for subsequent sequencing experiments.....	50
Figure 11. Sanger sequencing chromatograms of cloned <i>OsPDS</i> amplicons show deviations between replicates within a single sample. Sequences not consistent with the wild type <i>OsPDS</i> gene could be indicative of a gene edit. Alignment created using Benchling.com.....	51
Figure 12. Synthego's ICE tool analysis of Sanger sequencing results for sgRNA1 (A) and sgRNA2 (B). Samples with 5% indels or fewer, delineated by vertical grey line, were disregarded. Efficiency is defined as the percent of the sequence pool that deviate from the wild type sequence for each sample. Knockout-score represents the proportion of samples that have either a frameshift or indel greater than 21 bp.....	52
Figure 13. Synthego ICE sequencing data from individual trace files returned from Sanger sequencing. A, B: sequences present in the edited population and their relative proportions. Expected cut sites (three bp upstream the PAM) are represented by black vertical dotted lines, and the wild type sequence is marked by the orange "+" symbol. C, D: Edited vs wild type chromatograms in the region around the guide sequence. Guide sequences are underlined in black, the PAM site is underlined red, and the vertical black dotted line depicts the cut site. E, F: aberrant phenotypes of treated seeds that were sent for Sanger sequencing. Overall <i>OsPDS</i> gene model from MSU Rice Genome Annotation database.	53
Figure 14 A. Trimmed NGS sequence files were analyzed in CRIS.py software for each sgRNA. Intact, unedited sgRNA target regions are highlighted in yellow. In this sample, 1,950 reads (of 201,314 total) were edited within the sgRNA cut site, a nearly 0.97% editing efficiency. B. Aligning the most frequent mutant read to the <i>OsPDS</i> wildtype sequence shows a single	

nucleotide substitution within the sgRNA2 target region of Exon 3. PAM sequence is underlined.	54
Figure 15. <i>Gossypium</i> pollen grains after 5.5 hours on Burke et al.'s cotton pollen germination medium. Pollen grains were incubated at exact pH, humidity, temperature, and media requirements specified, yet no pollen tubes germinated.	62
Figure 16. <i>Gossypium</i> pollen grains after 20 hours on Dickinson et al.'s <i>Arabidopsis</i> pollen tube germination medium. Even at optimal temperature and humidity conditions specified for cotton by Burke et al., 2004, no pollen tubes had formed.	63
Figure 17. Improvement of pollen tube germination media over a span of several months. Monthly progressions show increased germination frequency and tube length after three-hour incubation. Images depict pollen grains of different <i>Gossypium</i> species. B. Media components and preparation methods.	65
Figure 18. Comparison of pollen tube germination on final working medium between <i>Gossypium</i> cultivars. Though pollen tube length differed greatly between genotypes, germination efficiency remained relatively constant.	67
Figure 19. Effect of MES CNT-delivery buffer on pollen grains and pollen tubes. <i>Gossypium</i> pollen grains were placed on working germination medium at optimal environmental conditions, and 50 uL of MES was added to plates either before incubation (A) or after a one-hour incubation (B). Images were taken two hours after initial plating. Cytoplasmic debris can be seen exuding from pollen grains treated with MES. By comparison, green arrows indicate intact pollen tubes in an untreated control (C).	68
Figure 20. Effect of MES buffer osmolarity on <i>Gossypium</i> pollen tubes and pollen grains <i>in vitro</i> . Sucrose was dissolved in MES at 10% increments to increase osmolarity and identify isotonic conditions. 50 uL of each solution was added to each plate one hour post-incubation, and images were taken after another one-hour incubation. Cell rupturing was observed in all treated samples. Intact pollen tubes are indicated by green arrows.	69

LIST OF TABLES

	Page
Table 1 List of Reporter Genes	24
Table 2 List of Gene Editing Plasmids	46
Table 3. Cotton Pollen Germination Media Components and Preparation Methods	66
Table 4 Primers used for PCR amplification. Primer sets used for Illumina NGS library adapter PCR do not include adapter sequences.	83

1. INTRODUCTION

The global population has been projected to reach ten billion by the year 2050, such that food production must increase by 70% on less total arable land to sustain the human population (FAO, 2017; United Nations, 2015). It remains an essential challenge to increase crop yield, resilience, and nutrition if we hope to achieve global sustainability. Crops have been improved by selection and traditional breeding, but additional methods are needed, preferably faster, more precise, and less reliant on chance. Advancements in gene editing hold great promise in helping us meet global crop demands within a reduced timeframe (Chen et al., 2019; Scheben et al., 2017). While gene editing has proven relatively successful in animal cells, current methods in plants, however, are far from fully optimized due to cell walls barring delivery of CRISPR components, difficult plant regeneration, genotype-specific protocols, and unpredictable off-target effects (Altpeter et al., 2016).

Our research aims to optimize a gene editing system that avoids tissue regeneration and random gene integration altogether. Carbon nanotubes (CNTs) designed by Demirer, Zhang, Matos, et al. (2019) of UC Berkeley have been shown to passively diffuse through plant cell walls and, when loaded with plasmid DNA (pDNA) cargo, can aid in transient expression of foreign DNA in plant cells. CNTs can potentially provide a passive, nondestructive mechanism to transform mature plant embryos with clustered regularly interspaced short palindromic repeats (CRISPR) mechanisms to make precise genetic alterations in germline precursor cells. Gene

alterations could be subsequently inherited in progeny, creating a generation of plants with desired gene edits. CNT-mediated gene editing in the germline cells could obviate the need for *in vitro* tissue regeneration and would prospectively be applicable to a wide range of species, offering an ideal platform for gene editing.

1.1. CRISPR Systems for Gene Editing

CRISPR and CRISPR-associated (Cas) protein act together as a bacterial immune response that recognizes and cleaves specific viral sequences in a form of acquired immunity (Makarova et al., 2011; Marzec et al., 2020). CRISPR immunity involves three distinct mechanisms: adaptation, expression, and interference (Makarova, 2015). In the adaptation stage, bacteria integrate targeted viral sequences into their own genome, creating a linear array of spacers (Barrangou et al., 2007). Transcription of CRISPR arrays produce CRISPR RNA (crRNA) and trans-CRISPR RNA (tracrRNA) that together form a complex with Cas nucleases, such as Cas9, during the expression stage (Deltcheva et al., 2011, Makarova et al., 2015). Finally, during the interference stage, the RNA-Cas nuclease complex cleaves sequences complementary to the crRNA, thereby impeding infection by identifying and targeting returning pathogenic invaders (Barrangou et al., 2007, Brouns et al., 2008). The natural system of crRNAs and tracrRNAs has been modified into a single-guide RNA (sgRNA) that could easily be modified to target specific sequences and cause breaks in double-stranded DNA (Jinek et al., 2012).

The ability of CRISPR/Cas systems to induce targeted double-stranded breaks in host DNA makes it a powerful tool for gene editing. Altered cells have the innate ability

to repair DNA breaks by two mechanisms: non-homologous end joining (NHEJ) or homology directed repair (HDR) (Sander & Joung, 2014). The two repair mechanisms are useful for precise gene editing: NHEJ creates small insertion/deletions (indels) that can disrupt gene reading frames or modify promoter sequences, while HDR can enable point mutations, insert new sequences, or allow for allele replacements. CRISPR/Cas specificity can also direct precise single-base substitution, methylation, and acetylation through the use of fusion proteins with a deactivated Cas9 (Chen et al., 2019; Kungulovski & Jeltsch, 2016; Marzec et al., 2020). CRISPR's precision and versatility can expand fields such as biological pharmaceuticals (Chen & Lai, 2015), gene therapies (Ledford, 2019), and bioenergy (Himmel et al., 2007), making it a universally essential tool in biotechnology.

1.2. Current CRISPR Delivery Methods for Gene Editing in Plants

Delivery of CRISPR systems still poses a challenge when editing the genome of organisms with cell walls such as plants: methods are labor-intensive and imprecise. For instance, *Agrobacterium tumefaciens*-mediated transformation involves unpredictable integration of transgenes, which face tight regulations worldwide (Turnbull et al., 2021). Biolistic approaches like particle bombardment can also be used for plant transformation but are unpredictable and often lead to off-target effects due to cell damage and random integration of DNA fragments (Liu et al., 2019). The level of genome damage ranges from small fragment displacement to chromosome truncations, both of which can greatly impede transformation efficiency and reliability.

Additionally, *Agrobacterium*-mediated and biolistic transformations often involve time-consuming *in vitro* tissue culturing and regeneration that considerably prolong the gene editing pipeline (Banakar & Wang, 2020; Hwang et al., 2017). Transformation protocols involving callus induction are genotype-dependent and pose a cumbersome, lengthy endeavor: plant regeneration from callus takes several months for rice (*Oryza sativa*) even under optimal conditions (Karthikeyan et al., 2009; Wardrop et al., 1996). The low survival rate of regenerated plantlets during the transplanting process further reduces transformation efficiency (Yang et al., 2017). Circumventing tissue regeneration would both facilitate and expedite the transformation process while also expanding gene editing to a broader range of cultivars.

1.3. Gene Editing with Nanoparticles

CNTs offer a precise, transgene-free gene editing system that avoids transgene regulations. With dimensions as low as 4 nm x 0.5 μ m, nanotubes fall below the size exclusion limit of plant cell walls and membranes, allowing them to enter undamaged cells by diffusion through cell walls and penetration through plasma membranes (Demirer, Zhang, Matos, et al., 2019). The reporter DNA cargo loaded onto CNTs can be transcribed for several days post-infiltration, proving DNA fragments are able to passively enter cell nuclei when electrostatically grafted to CNTs. Reporter gene expression is transient and diminishes after about ten days post-infiltration (Demirer, Zhang, Matos, et al., 2019). CNTs can therefore act as a transport mechanism to shuttle CRISPR/Cas machinery into plant cells to create a transient, non-integrative gene editing system. Such a system could directly alter germline cells through *in planta*

transformation, eliminate the challenge tissue regeneration, and present a genotype-independent method for rapid crop improvement of a wide range of plants.

1.4. Phytoene Desaturase

The phytoene desaturase (*PDS*) gene is a useful target to optimize gene editing: disruption results in albino and dwarf phenotypes (Qin et al., 2007). For rice, the MSU Rice Genome Annotation database of *Oryza sativa* gene references can be used to identify genes for targeted knockout (Kawahara et al., 2013). *PDS* encodes an oxidoreductase that converts phytoene into zeta-carotene, thus playing a vital role in biosynthesis of photosynthetic pigments (UniProt, 2019). Rice phytoene desaturase (*OsPDS*) will be targeted for knockout because *pds* mutations are nonlethal, have been replicated by *Agrobacterium*-mediated transformation, and produce an easily recognizable dwarfed-albino phenotype that acts as a visual indicator of successful gene editing (Decaestecker et al., 2019; Xu et al., 2017). sgRNAs complementary to MSU's 5.7 kb *OsPDS* (LOC_Os03g08570.1) sequence from *O. sativa subsp. japonica* can be designed and verified *in vitro* for use in subsequent gene knockouts experiments. *OsPDS* knockout genotypes can be aligned to the wildtype LOC_Os03g08570.1 sequence on the MSU database to assess indels (Kawahara et al., 2013).

1.5. Pollen Tubes

The delivery of sperm cells to female gametophytes is crucial to sexual reproduction in flowering plants. Sperm cells are delivered down the style through elongating structures called pollen tubes, which emanate from individual pollen grains upon contact with viable stigmatic tissue. A pollen grain will land on the stigmatic

surface of a pistil, hydrate, and germinate to form a pollen tube. Localized cell wall elongation into the style transports two sperm cells toward the female gametophyte for fertilization (Edlund et al., 2004; Krichevsky et al., 2007). The cell wall at the tip of the elongating pollen tube is composed of a single layer of pectin (Chebli et al., 2012; Ferguson et al., 1998). As opposed to the multilayered, polymerized pollen coat, the single-layered cell wall of the elongating pollen tube would seem to provide a favorable point of access for CNT diffusion. Nanoparticle-mediated gene delivery was successful in germinating palm oil pollen grains (Lew et al., 2020). However, transformation of pollen tubes from other plant species, especially economically important dicots such as cotton, has not been thoroughly examined. Transgenic pollen tube transformation has been previously documented in cotton, validating predictions that CNT-mediated transformation is possible (Wang et al., 2019). Pollen tubes grown *in vitro* should facilitate gene editing with CNTs due to increased, uniform surface area of the *in vitro* substrate. Furthermore, the ability to fertilize stigma with pollen tubes grown *in vitro* has been documented in *Arabidopsis* (Dickinson et al., 2018), alluding to the possibility of fertilizing receptive flowers with CNT-edited sperm cells to create gene edited seeds. Recent results provided preliminary evidence of this ability in cotton, too (Stelly, personal communication, October 23, 2021).

1.6. Rationale and Objectives

While other prominent methods for gene editing in crops have been well-documented, each presents its own shortcomings and limitations. The two major techniques used today, *Agrobacterium* infiltration and particle bombardment, both

involve *in vitro* tissue regeneration to achieve stably gene-edited plants. Whole-plant regeneration is often an inefficient, rate-limiting step of the gene editing pipeline, which this research seeks to circumvent: CNTs bypass tissue culturing by promoting transient transformation of intact plant tissues including meristems and germline precursors.

Successful transformants can be initially detected using yellow fluorescent protein (YFP) and green fluorescent protein (GFP) visual reporter genes. Rice plants transformed with CRISPR systems targeting *OsPDS* will allow for visual assessment of gene editing. *OsPDS* loss-of-function can be recognized visually by tissue-specific reduction of green pigmentation due to knockout of synthesis pathways and can be further confirmed by Next Generation Sequencing (NGS). Illumina MiSeq NGS can identify heterozygous and chimeric edits by providing quantitative mutant read counts, which could also elucidate transformation efficiency. Visual and molecular data should indicate if transient transformation of plants by passive diffusion using CNTs has been achieved and establish a testing platform that would enable optimization of CNT-based gene editing protocols.

Optimization of an *in vitro* cotton pollen tube system could lead one step closer to developing another method of germline editing that also bypasses tissue culture complications. Though beyond the scope of this study, the protocol developed here could eventually be combined with CNT experiments, transferring transformed sperm onto stigma and giving rise to gene edited progeny.

In order to optimize delivery and transformation with CRISPR/Cas9 gene editing components, the following objectives were pursued:

1. Verify CNT capacity to deliver plasmids into rice leaf tissues using visual reporter genes.
2. Assess CNT ability to transport gene editing plasmid vectors into early rice embryos and induce gene edits.
3. Determine whether these gene editing methods can be used to transform cotton pollen tubes, which should be more receptive to CNT diffusion when exposed from the pollen coat.

2. TRANSIENT EXPRESSION OF REPORTER PLASMIDS IN RICE TISSUES BY CNT INFILTRATION

2.1. Synopsis

Initial studies of CNTs report their passive diffusion in intact monocot and dicot leaves. These transient infiltration events, however, have not been tested in rice. Reporter plasmids encoding fluorescent protein or GUSPlus genes were electrostatically bound to CNTs for infiltration of rice leaves, seeds, and mature embryos. Transient expression of reporter genes acted as visual indication of effective CNT diffusion through intact cell walls as well as successful transcription and translation of foreign genetic elements from within the plant cells.

2.2. Introduction

CNT capacity to passively transport pDNA cargo *in planta* has been documented by Demirer, Zhang, Matos, et al., (2019), but not in rice. In this section, findings provide strong evidence verifying CNT ability to transport reporter plasmids into mature rice leaves and seeds. Successful transport has been identified by visual cues specific to each reporter gene: fluorescent proteins (GFP and EYFP) or GUSPlus. We aimed to optimize pDNA:CNT ratios, vector size, imbibement duration, and gene promoter for transient expression *in planta*. Plasmid DNA loaded onto CNTs was transcribed and translated, proving valuable for downstream efforts to transport CRISPR gene editing vectors for *in planta* gene editing.

2.3. Materials and Methods

2.3.1. pDNA-PEI-CNT Preparation

PEI-CNTs were prepared as directed by the protocol from Demirer, Zhang, Goh, et al. (2019) to functionalize the CNTs in preparation for attachment of the plasmid DNA. Briefly, single-walled, carboxylic acid functionalized carbon nanotubes (Sigma-Aldrich cat. no. 652490) were first covalently modified with the cationic polymer polyethylenimine (PEI, branched, molecular weight 25,000; Sigma-Aldrich cat. no. 408727) to carry a net positive charge in preparation for attaching plasmid DNA. Following the published protocol, zeta potential was measured by Zetasizer Nano ZS and determined within the appropriate +50 to +70mV range before continuing. Fresh PEI-CNTs were stored in aliquots at 5 °C and prepared fresh every month or until agglomeration of nanoparticles became visible to the naked eye.

Fresh pDNA was electrostatically grafted to PEI-CNTs following the protocol of Demirer, Zhang, Goh, et al. (2019). Chilled CNT aliquots were brought to room temperature 30 minutes prior to a 45-minute bath sonication to thoroughly resuspend nanoparticles. CNTs were diluted to appropriate concentrations in 2-(N-morpholino)-ethanesulfonic acid (MES) delivery buffer. pDNA-PEI-CNT solutions were prepared in varying pDNA-to-CNT ratios ranging from 6:1 to 1:3. Activated PEI-CNTs were added to pDNA at least 30 minutes prior to use in experiments.

2.3.2. Transformation Vectors

Reporter plasmids ranged in size from nonbinary vectors fewer than 3.7 kb to binary gene editing vectors nearly 13.7 kb. Eleven main reporter plasmids were tested to visualize CNT transformation (Table 1).

Table 1 List of Reporter Genes

Vector Backbone	Reporter Gene	Promoter	Size (kb)
pCAMBIA1305.1 (binary)	GFP, GUSPlus	CaMV 35S	13.7
pTRANS210 (binary)	GFP	ZmUbi	12.1
pPTN (binary)	EYFP	ZmUbi	12.0
pCAMBIA1305.1 (binary)	GUSPlus	CaMV 35S	11.8
pTRANS210 (binary)	GFP	CaMV 35S	10.9
pTRANS210 (binary)	GFP	CmYLCV	10.5
pUC19 (nonbinary)	GUSPlus	CaMV 35S	5.4
pTRANS100 (nonbinary)	GFP	ZmUbi	5.2
pENTR (nonbinary)	Nuclear-Localized GFP	EL2	5.1
pTRANS100 (nonbinary)	GFP	CaMV 35S	4.0
pTRANS100 (nonbinary)	GFP	CmYLCV	3.7

2.3.3. Leaf Infiltrations with CNTs

Maturing Nipponbare and Presidio rice plants were grown in a Conviron chamber under long day conditions (14-hour light, 10-hour dark cycles at 29 °C and 25% relative humidity) until at least three true leaves had emerged. Leaves were mechanically

wounded with needles and soaked in pDNA-PEI-CNT solution as described for monocot leaf infiltration (Andrieu et al., 2012). Binary and nonbinary pDNA vectors encoding EYFP, GFP, or GUSPlus driven by different constitutive plant promoters, as depicted in Table 1, were infiltrated into the leaves. Plants were kept at room temperature and ambient lighting during infiltration to preclude possible breakdown of fluorescent proteins under extreme light conditions (Tamura et al., 2003). Fluorescence was observed under Echo Revolve and Olympus SZX10 light microscopes, and GUS enzymatic activity was visualized by histochemical assay (Cervera, 2004) following 24-hour intervals post-infiltration.

2.3.4. CNT Infiltration of Rice Seeds with Reporter Plasmids

Prior to treatment with CNTs, mature desiccated Nipponbare seeds were surface sterilized in a 70% ethanol solution for three minutes followed by a 4.5% bleach wash for 35 minutes. Seeds were thoroughly washed five times with autoclaved deionized water to remove bleach. To initiate germination, surface-sterilized seeds were placed in a petri dish, covered with sterilized water, and incubated overnight at 29 °C.

Rice seeds were first imbibed in a 0.6 M mannitol solution for two hours to decrease osmotic pressure within the plant tissues. Seeds were then dried on sterile filter paper before submergence in pDNA:CNT solutions at varying ratios. Plasmids were covalently attached to positively charged CNTs at least 30 minutes prior to use. Seeds were vacuum-infiltrated at 500 mm Hg for five minutes in CNT solution before storing at 29 °C on a 14-hour light, 10-hour dark cycle. Images were taken at 24-hour intervals by Olympus SZX10 stereomicroscope and Echo Revolve light microscope.

2.3.5. CNT Infiltration of Shoot Apical Meristems with Reporter Plasmids

Mature embryos were excised from select sterilized seeds. Shoot tips were cut away to reveal shoot apical meristems (SAMs) and the embryo cut away from the endosperm using a fine-point scalpel. Such methods have been previously employed to facilitate production of transgenic plants (Dutt et al., 2007; Sato et al., 1993). Excised embryos were placed in a 0.6 M mannitol osmotic solution for two hours prior to imbibement in reporter pDNA-CNT solutions following the methods described in Section 2.3.4.

2.3.6. Fluorescent Transcript Confirmation

Emission data for fluorescence was quantified by ImageJ following instructions from University of Maryland, Baltimore County (n.d.): background fluorescence was subtracted from integrated density around the treated area. Corrected fluorescence for each leaf was averaged over at least three samples and sorted by number of days in solution. Statistical differences in fluorescence were determined by Tukey's Honestly Significant Difference (HSD) test.

Next, GFP and EYFP expression was confirmed via reverse transcription PCR (RT-PCR) analysis: fluorescing leaves were excised and immediately frozen by liquid nitrogen. A SPEX 1600 MiniG plate homogenizer was used to grind leaf tissues into a fine powder before extracting RNA following instructions from a Qiagen RNeasy Plant Mini Kit. RNA was treated with DNase and complementary DNA (cDNA) was synthesized with an Invitrogen SuperScript™ III First-Strand Synthesis System and oligo(dT) primers. Resulting cDNA was treated with RNase prior to PCR amplification

(KAPA3G Plant PCR Kit, Kapa Biosystems) with transcript-specific primers. All primer sequences can be found in Table 4 of the Appendix. PCR products were run on a 1.2% agarose gel to visually confirm presence or absence of amplicons indicative of GFP or EYFP transcripts in leaf extracts.

2.3.7. Confocal Imaging of Nuclear-Localized GFP

Binary plasmids encoding a plant-specific nuclear-localized GFP were also tested with CNT infiltration of rice leaves and embryos. As fluorescence localized to the nucleus could not be determined by Olympus SZX10 or Echo Revolve microscopes due to low resolution, tissue samples were brought to the Texas A&M (TAMU) Microscopy and Imaging Center (MIC) for hand-sectioning, staining, and imaging of both leaf and embryo samples. Nuclei were stained with DRAQ5 to delineate plant nuclei according to Smith et al., 2004, and images were taken under a Leica Microsystems SP8 confocal microscope.

2.3.8. GUSPlus Transcript Confirmation

We confirmed GUSPlus expression in transformed tissues in a fashion similar to Section 2.3.6: leaves treated with GUSPlus vectors and CNTs were ground into a fine powder and processed by Qiagen RNeasy Plant Mini Kit and Invitrogen SuperScript™ III First-Strand Synthesis System. cDNA was PCR amplified with GUSPlus-specific primers. Primers specific to the housekeeping gene LOC_Os03g08020 encoding RICE ELONGATION FACTOR1-ALPHA-LIKE (EFA) were used to amplify cDNA as a positive reverse-transcription control. We separately amplified cDNA by PCR with primers specific to the selective marker of the plasmid backbone as a control ensuring

proper DNase treatment. PCR products were run on a 1.2% agarose gel to visually confirm presence or absence of amplicons indicative of GUSPlus transcripts in leaf tissues.

2.4. Results

2.4.1. Transient Fluorescence in Rice Leaves and Embryos

Leaves were infiltrated with pDNA-CNTs suspended in MES delivery buffer at concentrations of 1.5 ng pDNA per μL and at ratios ranging from 6:1 to 2:1 pDNA:PEI-CNTs. Images were taken under an Olympus SZX10 stereomicroscope with a single GFP filter set after three days in solution. Initial experiments found that GFP driven by the CmYLCV promoter triggered significantly more fluorescence than when driven by CaMV 35S or ZmUbi (data not shown). Thus, all following experiments involving GFP took advantage of the CmYLCV promoter.

Increased fluorescence can be seen from the 2:1 ratio samples with GFP driven by the CmYLCV promoter compared to the CNT-only control and the plasmid-only control (Figure 1). A comparison across the 2:1, 4:1, and 6:1 ratios of plasmid DNA to CNTs showed that the 2:1 ratio had the highest level of fluorescence (Figure 2). These results suggest that the plasmid DNA was delivered into the rice leaf cells by the CNTs, and then transcribed and translated in the cells, leading to the fluorescent signal from the GFP reporter gene.

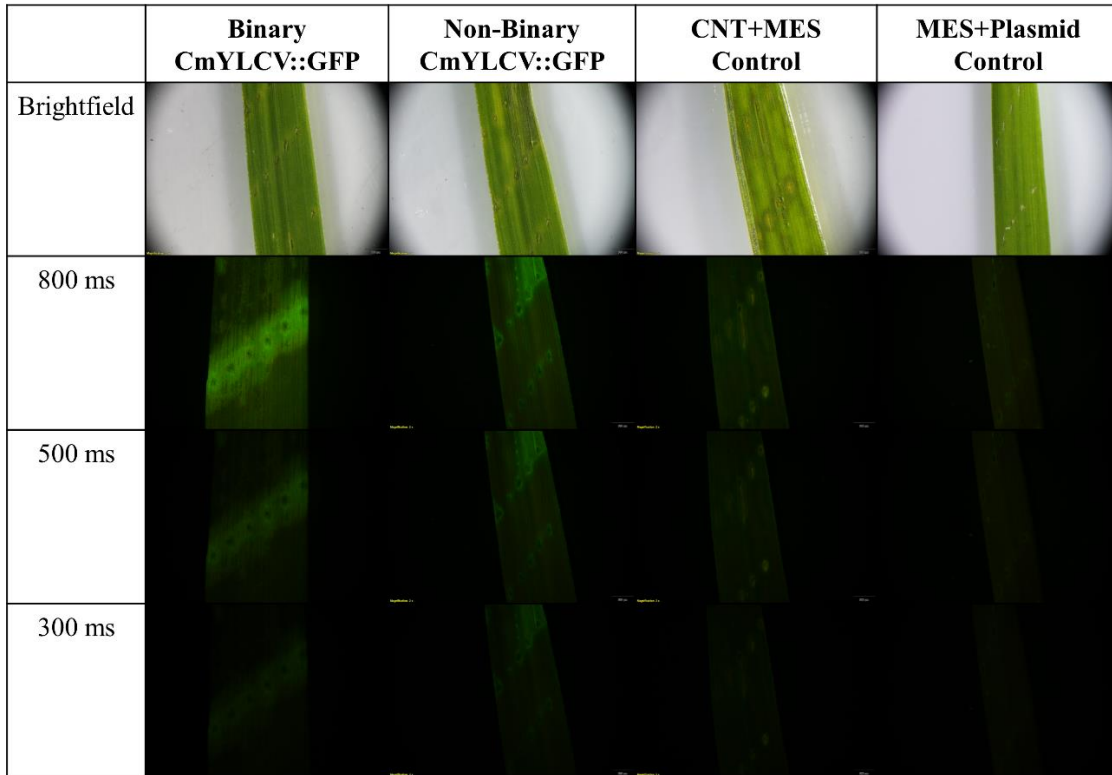


Figure 1. Brightfield and fluorescence stereomicroscope images of rice leaves infiltration using binary and nonbinary plasmid vectors encoding GFP driven by CmYLCV promoters. CNT solution consists of a 2:1 pDNA:CNT ratio. Leftmost columns indicate exposure time.

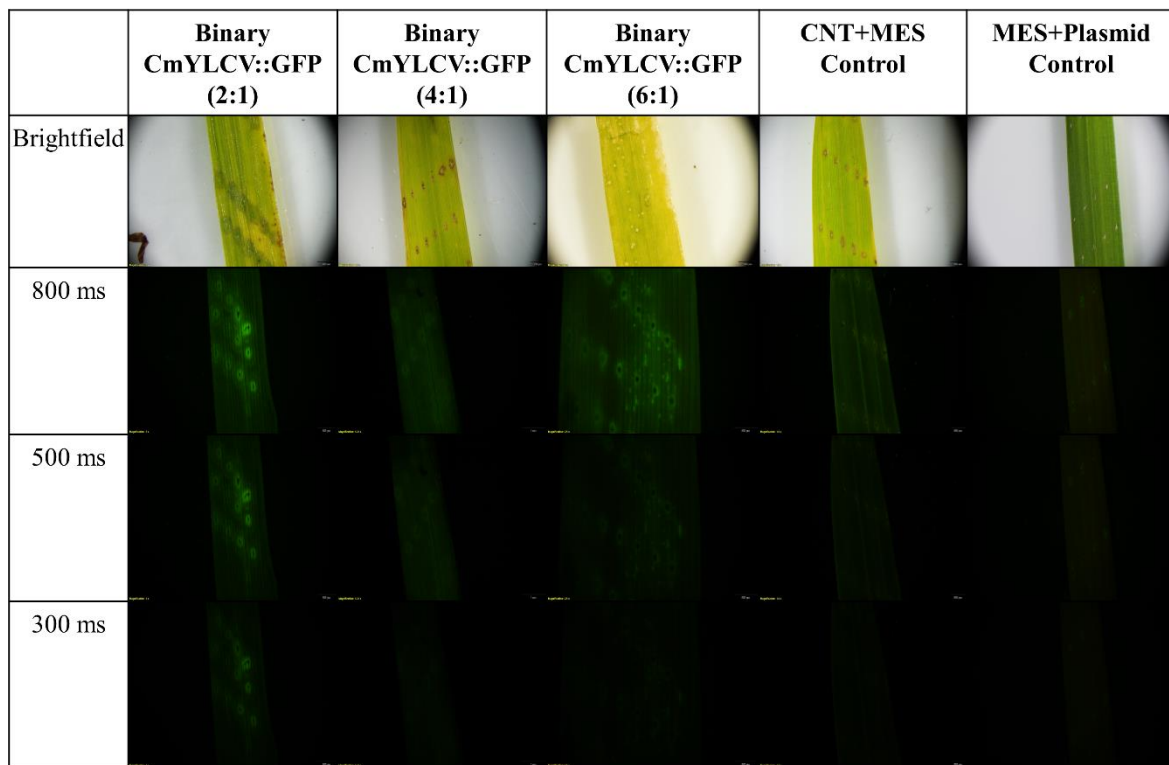
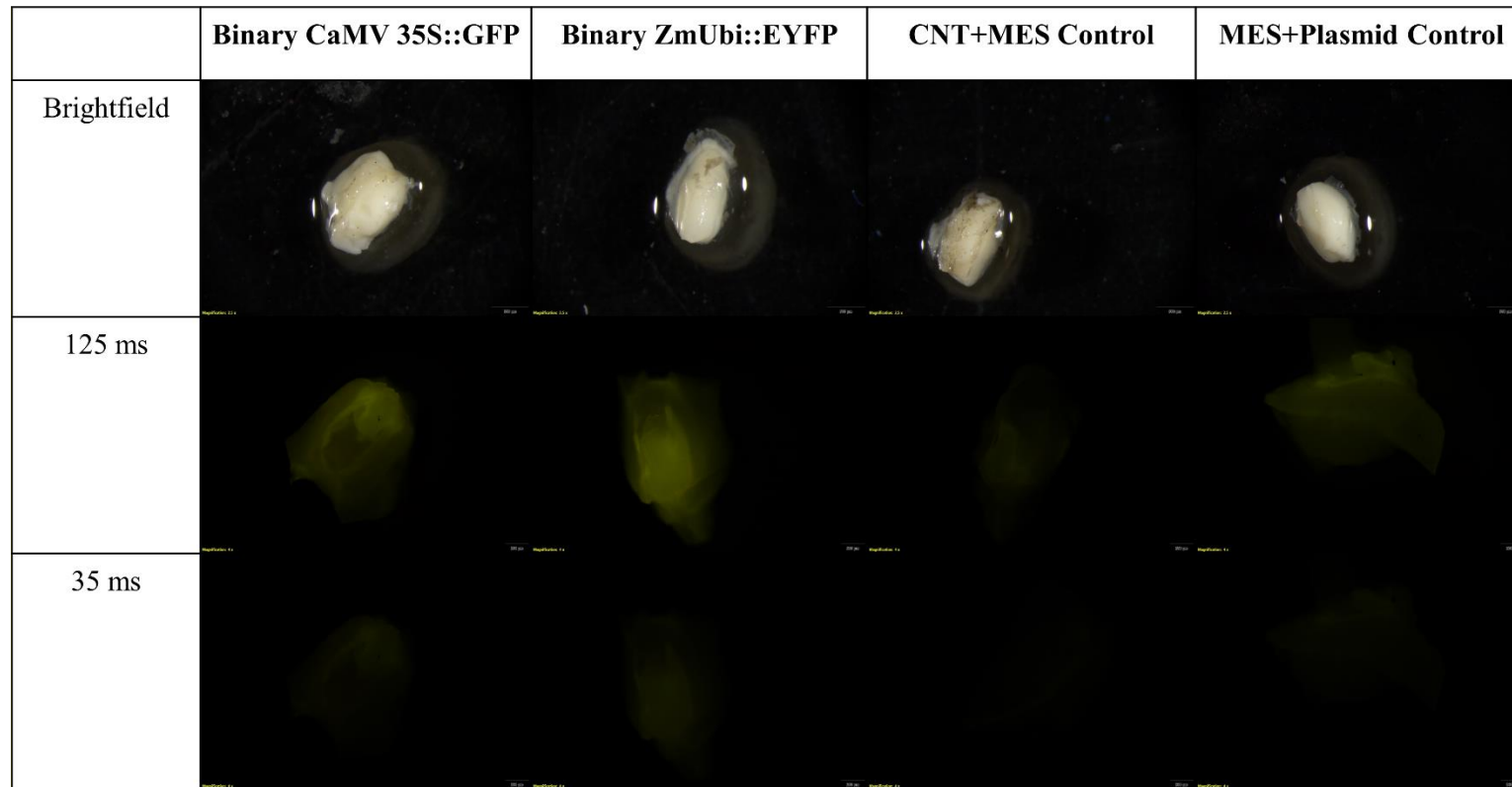


Figure 2. Brightfield and fluorescence stereomicroscope images of rice leaves three days post-infiltration with binary CmYLCV::GFP pDNA-CNT solutions at 2:1, 4:1, or 6:1 pDNA:CNT ratios. Leftmost columns indicate exposure time.

Similarly, excised embryos were imbibed in pDNA-CNT solutions for three days prior to viewing fluorescence under the microscope. Although there was some background fluorescence in the control samples, a clear increase in fluorescence can be seen in the samples imbibed with CNTs attached with CaMV-GFP and ZmUBI-EYFP plasmids at a 1:3 ratio of plasmid DNA to CNTs (Figure 3A). Moreover, RT-PCR with GFP-specific primers on a subset of fluorescing samples showed three out of three excised embryo (shoot apical meristem) samples showing a positive product, while four out of six whole seeds tested positive for GFP transcripts. Similarly, three out of five

excised embryos and three out of three imbibed seeds tested positive for EYFP-specific primers (Figure 3B).

A



B

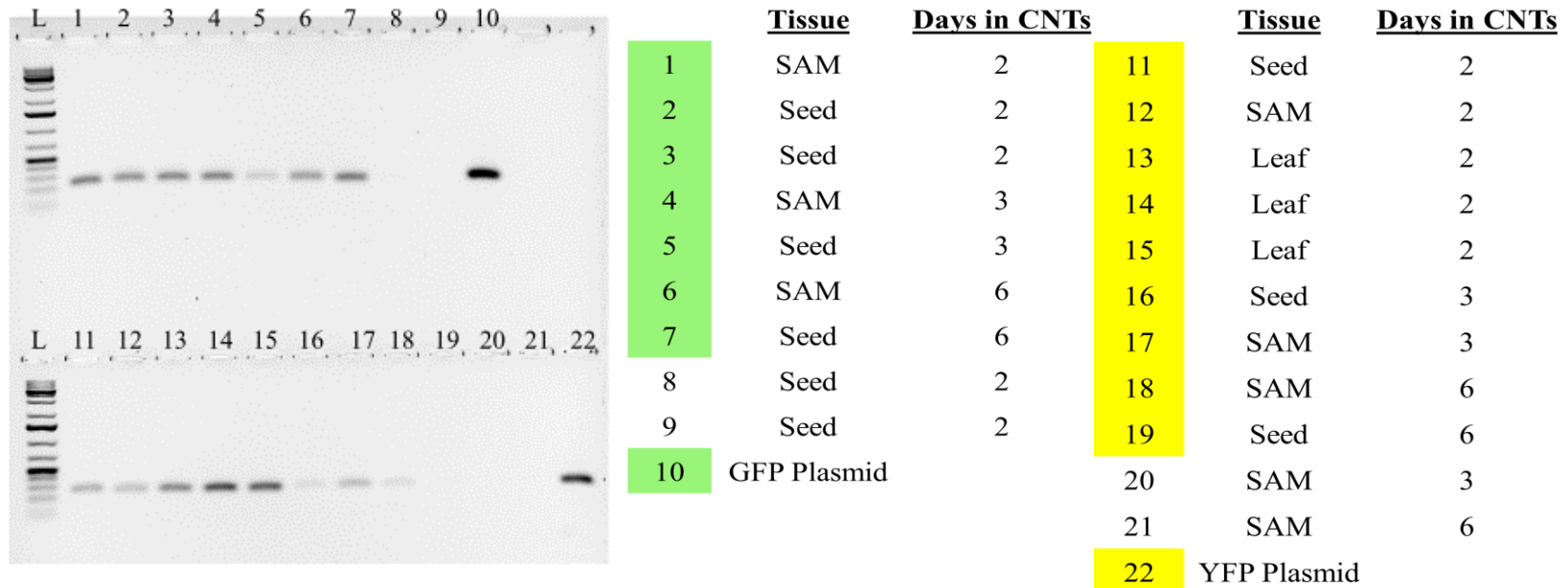


Figure 3 A. Brightfield and fluorescence stereomicroscope images of rice embryos three days post-imbibe with CaMV 35S::GFP- or ZmUbi::EYFP-CNTs compared to plasmid-only and CNT-only controls. Solutions consist of 1:3 pDNA:CNT ratios. Embryos were oriented to show maximum fluorescence. RNA was extracted and synthesized into cDNA, then amplified with GFP- or EYFP-specific primers following HF Phusion polymerase parameters. **B.** Products were run on a 1.5% agarose gel for 75 minutes at 50V. Ladder: GeneRuler 1kb Plus.

Integrated fluorescent density was determined using ImageJ, and corrected total fluorescence was calculated using formulas from the University of Maryland, Baltimore County (n.d.). Relative fluorescence levels of GFP were higher than controls for rice leaves treated for one and two days in solution, while YFP levels were significantly higher than controls after two and three days in solution (Figure 4).

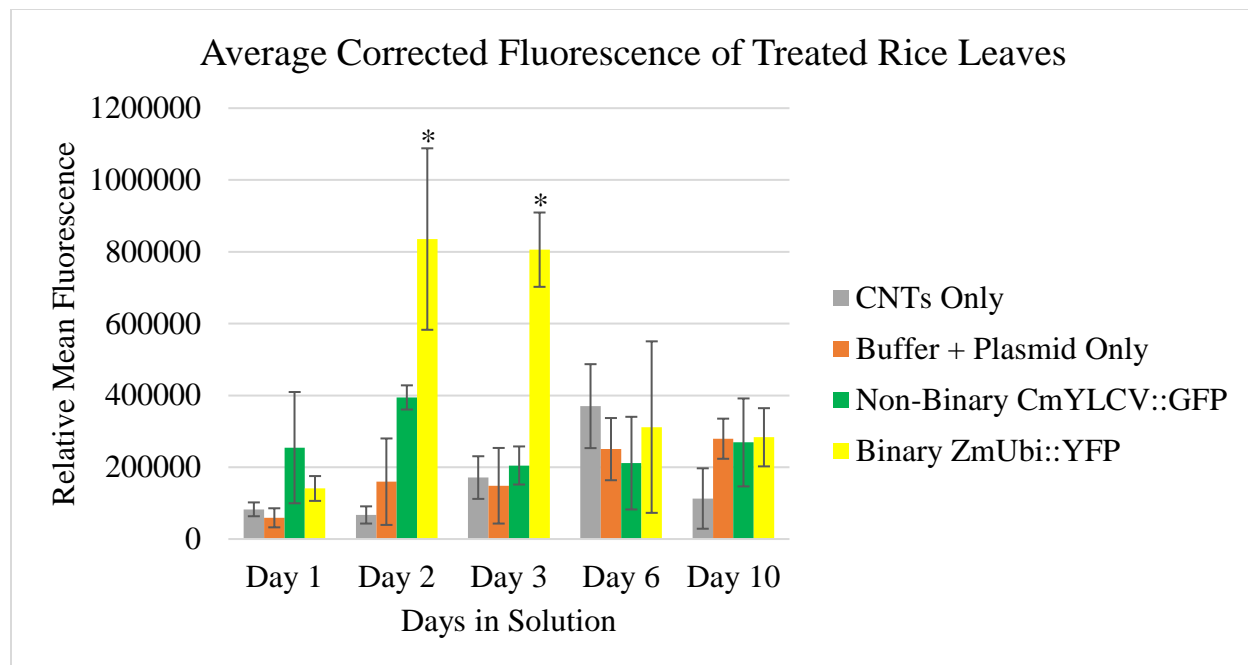


Figure 4. Average corrected fluorescence of rice leaves treated with pDNA-CNTs and imaged under stereomicroscope over a period of ten days. Corrected total fluorescence was determined by subtracting background fluorescence from the total fluorescence of the treated area (integrated density calculated by ImageJ). Asterisks indicate significantly different fluorescence determined by Tukey’s HSD.

2.4.1.1. Nuclear-Localized Fluorescence

To test whether a nuclear-localized GFP may provide more clear fluorescence signal over the background fluorescence, leaves and excised embryos infiltrated with a nuclear-localized GFP (NLS-GFP) grafted to CNTs were initially viewed and imaged under Olympus SZX10 and Echo Revolve microscopes after three days in solution, but results were inconclusive (Figure 5).

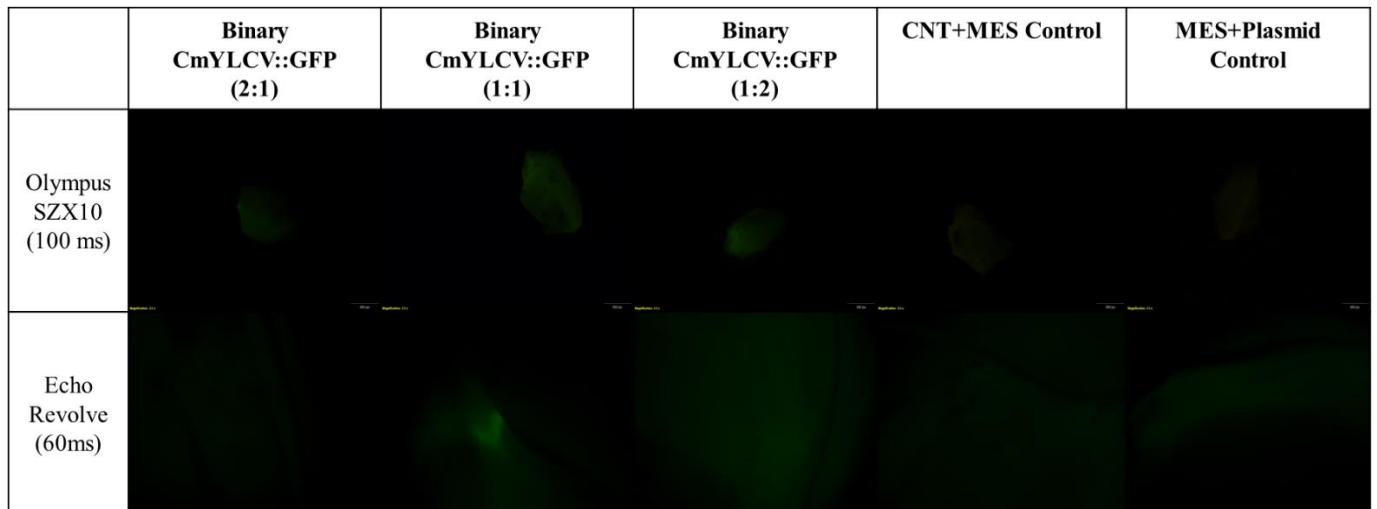


Figure 5. Excised embryos infiltrated with CNTs and NLS-GFP reporter plasmids were imaged under Olympus SZX10 and Echo Revolve stereomicroscopes after three days post-imbibe.

Individual cells were indistinguishable under our stereomicroscopes, and we required higher resolution microscopy to determine if fluorescence was truly localized to nuclei. Images of NLS-GFP-treated rice embryos and leaves were taken by confocal microscopy at the TAMU MIC. Results showed some nuclei with fluorescence indicating successful plasmid NLS-GFP delivery and expression, but some background fluorescence as well.

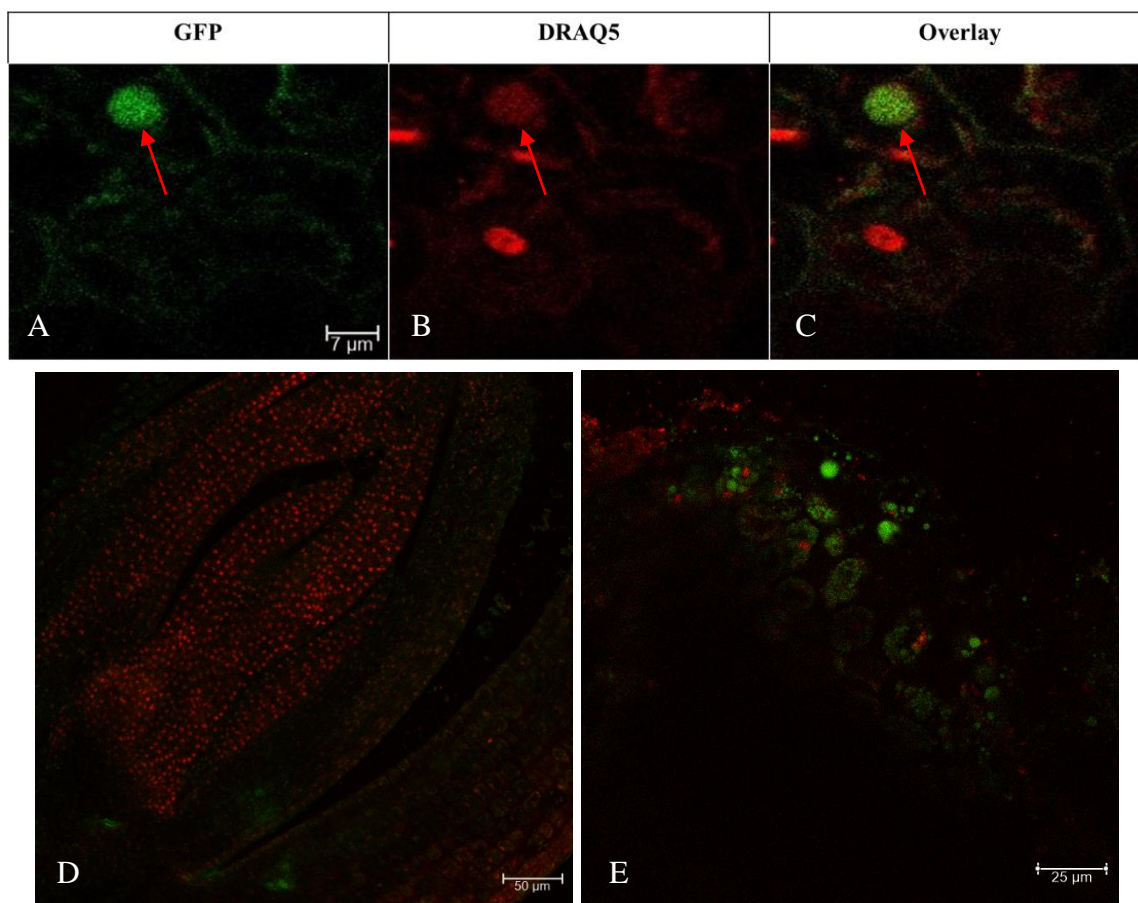


Figure 6. Excised leaves and embryos treated with CNTs carrying NLS-GFP vectors were sectioned, stained with DRAQ5, and imaged under confocal microscope after four days in solution. **A**, **B**, and **C** seem to indicate GFP fluorescence overlap with nuclear staining, but high levels of noise in negative controls (**D**) and unlocalized fluorescence in other treated samples (**E**) prevent us from drawing definitive conclusions. Sectioning and imaging performed by TAMU MIC.

2.4.2. Transient GUSPlus Expression

For the GUS assay, rice leaves and seeds were imbibed in the same fashion as with fluorescent reporter plasmids. However, endogenous GUS activity in rice seeds (Anbu & Arul, 2013) induced blue coloration in both experimental and negative control seeds alike, so follow-up experiments were only performed on rice leaf tissues. Following findings from previous experiments, leaves were imbibed for three days to allow a maximum accumulation of GUSPlus transcripts. Successful pDNA-CNT delivery into rice leaf tissue can be seen in the blue

coloration in the treated rice leaves compared to the controls (Figure 7). Likewise, GUSPlus-specific primers showed a band in an RT-PCR test, although only the non-binary GUSPlus plasmid showed a clear band (Figure 8).

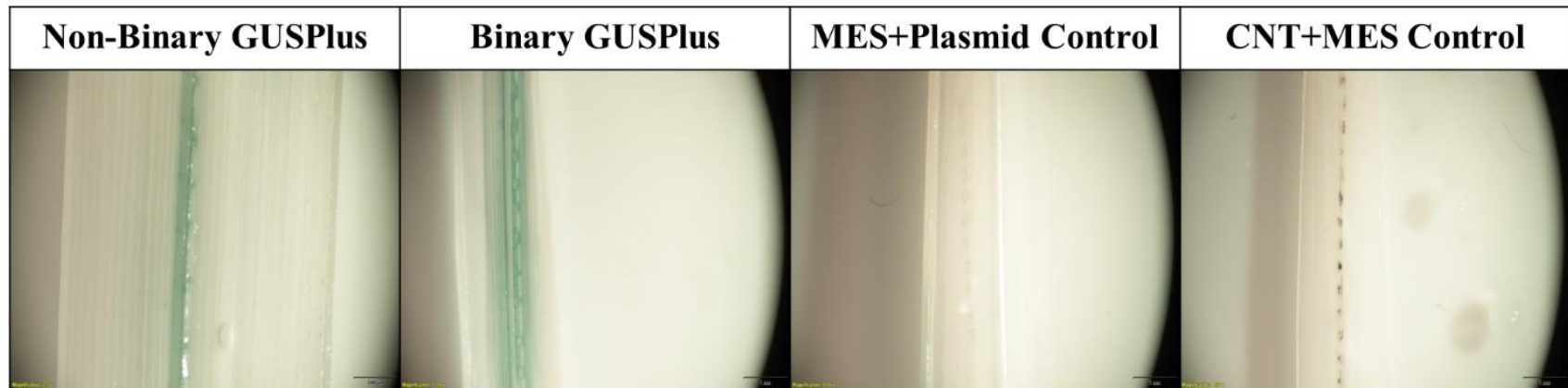


Figure 7. Rice leaves were punctured with needles and imbibed in CNTs loaded with GUSPlus vectors. After three days in solution, GUSPlus enzymatic activity was visualized by histochemical assay (Cervera, 2004) and chlorophyll bleaching. Blue coloration indicates GUSPlus activity in treated leaves at the infiltration site.

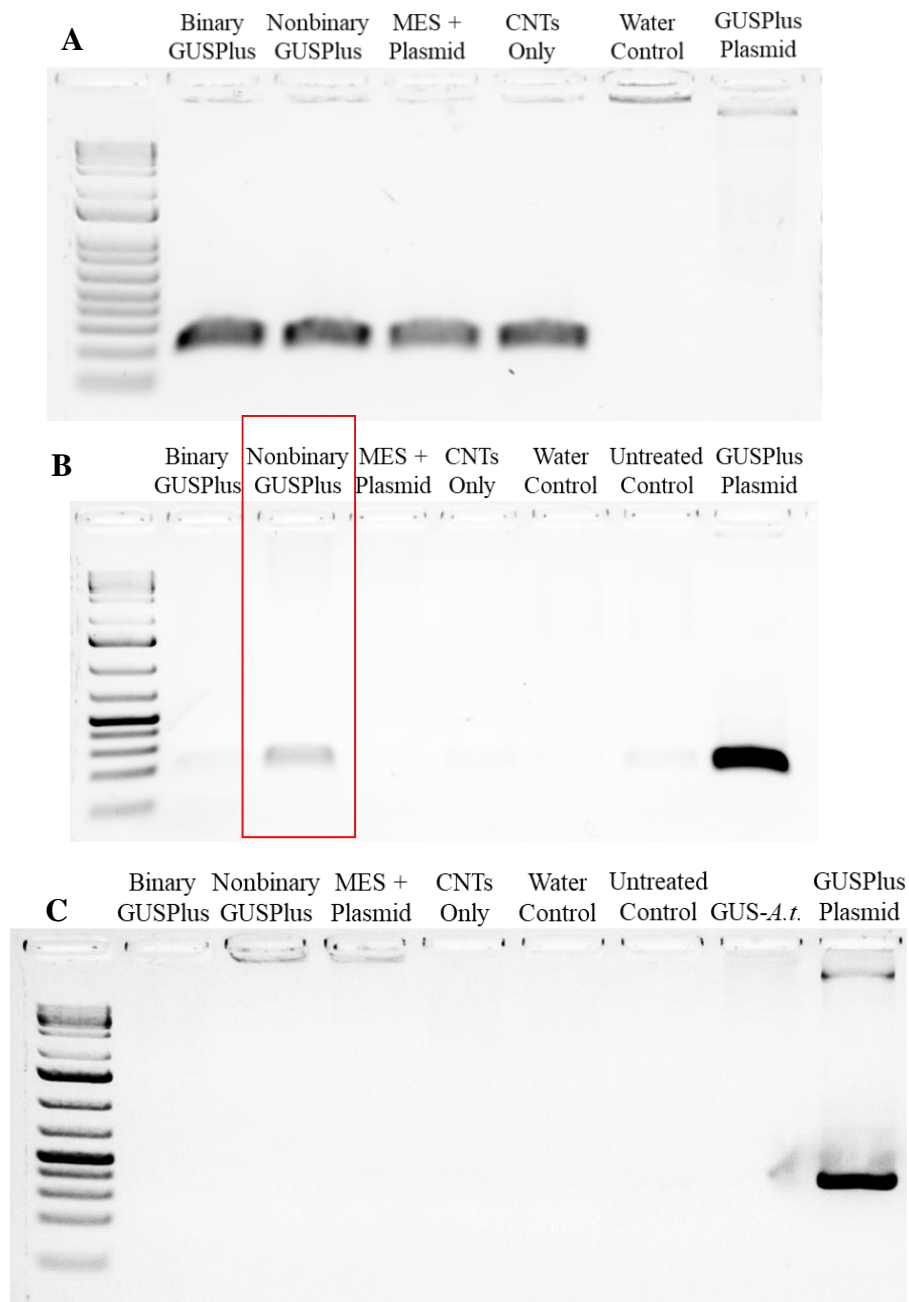


Figure 8. Oligo(dT) primers were used to synthesize cDNA from RNA extracted from GUSPlus-CNT treated rice leaves. **A.** Housekeeping primers specific to EFA were used to PCR amplify cDNA. Bands around 200 bp are indicative of successful cDNA synthesis from processed mRNA. **B.** Primers specific to GUSPlus were used to amplify a 160 bp fragment in the presence of GUSPlus transcripts **C.** Primers targeting the hygromycin resistance gene of the GUSPlus plasmid backbone amplified a 360 bp fragment only in the presence of residual pDNA.

2.5. Discussion

The experiments collectively evaluated a variety of fluorescent-reporter plasmids that differed in size, gene promoter (Table 1), and concentration relative to CNTs (Figure 2). Initial experiments found greatest fluorescence in leaves treated with CmYLCV::GFP (data not shown), and this cassette was used for all subsequent GFP infiltrations. Fluorescence imaging revealed signal from both binary and nonbinary CmYLCV::GFP-CNT-treated leaves—even at lowest (300 ms) exposure, whereas negative control leaves were nearly invisible (Figure 1). Note that binary vectors were originally developed for *Agrobacterium*-mediated transformation, but we used them here as a useful comparison to test if the plasmid size may impact the efficiency of CNT-mediated delivery into plant cells. Although one might logically anticipate that the small size of nonbinary vectors would facilitate passive movement into plant cells, nonbinary vectors did not produce visibly noticeable differences in fluorescence compared to binary plasmids driven by the same promoter.

We investigated three pDNA:CNT ratios (2:1, 4:1, and 6:1) for relative efficiency for leaves (Figure 2). Fluorescence was not obvious in leaves treated with the higher ratios of plasmid to CNTs. The lowest ratio, 2:1, produced the most fluorescence. While the 2:1 ratio lies nearly in the middle of the range presented by Demirer, Zhang, Goh et al. (2019), it might be that the optimal ratio for rice and our methods could be even lower. Additional experiments would be desirable.

We examined applicability of CNT passive diffusion into rice embryos using EYFP and GFP reporter genes. Assessments by imaging (Figure 1 and Figure 3A) and

transcript analysis (Figure 3B) strongly suggest transcription and translation of our reporter plasmids. Bands just over 200 bp in Figure 3B seem to indicate presence of GFP and EYFP transcripts in imbibed leaves, seeds, and embryos. Additionally, absence of amplification in negative control samples indicates lack of both fluorescent-protein transcripts and residual pDNA. However, cDNA synthesis was not verified by amplification of housekeeping genes, and this additional control should be included in replicate experiments.

Seeds imbibed in pDNA-CNT solutions were treated in the same way as excised embryos (targeting the shoot apical meristem), though little fluorescence was detected in seed samples. Because overall transcript analysis did indicate transcription of fluorescent protein mRNA across tissues, weak fluorescence may suggest either limitations of our microscopes or protein levels below levels of visual detection.

Transcription was indeed found to be transient in leaves as fluorescence diminished by ten days post-CNT imbibement. Figure 4 illustrates average levels of corrected fluorescence of imbibed leaves as measured by ImageJ software. Average fluorescence peaked at two to three days post-CNT treatment, with decreased standard deviation among samples on day three. YFP fluorescence is significantly greater than negative controls on days two and three days when running Tukey's Honestly Significant Difference Test. By day six, fluorescence decreases to near-baseline levels. These findings are in accordance with Demirer, Zhang, Matos, et al. (2019) and corroborate predictions of transient expression.

NLS-GFP fluorescence could not be traced strictly to the nucleus by either of our in-house Olympus or Echo Revolve fluorescent microscopes, as seen in Figure 5. Personnel of the TAMU MIC sectioned, stained, and imaged NLS-GFP-CNT treated leaves and embryos under confocal microscope. Due to unforeseen setbacks from COVID, samples were left at unfavorable conditions for an additional 24 hours and were not imaged until four days post-CNT treatment. This additional 24 hours could have led to increased background noise from contamination or plant stress responses. Furthermore, as NLS-GFP expression is transient, nuclear-localized fluorescence could have decreased by the fourth day. Although results of our NLS-GFP-CNT leaf and embryo imbibements were largely inconclusive due to high levels of fluorescent noise, at least one image looked promising for successful expression in the nuclei (Figure 6).

Binary and nonbinary vectors encoding GUSPlus enzymes were also used to visualize transient expression facilitated by CNTs. Imbibed leaves were fixed in formaldehyde, underwent Cervera's 2004 GUS histochemical assay protocol, and destained with ethanol. Images from Figure 7 were taken after 24 hours once all chlorophyll had been removed. Blue coloration indicative of GUSPlus enzymatic activity was only visible in GUSPlus-treated samples while negative controls remained colorless. Additionally, GUSPlus activity was only visible at the puncture sites where CNTs were able to infiltrate. These observations indicated positive GUSPlus expression, which we confirmed via transcript analysis.

RNA was extracted from treated rice leaves, and cDNA was synthesized for PCR amplification (Figure 8). Primers flanking the GUSPlus intron were designed such that

amplicons from residual pDNA would differ in size from true transcripts. If the gene were transcribed, the amplicon would not contain the intron and would be nearly 200 bp shorter than amplified pDNA that escaped DNase treatment. However, this primer set did not bind well, and we did not have a proper positive control with which to troubleshoot. We instead used a combination of primer sets to validate GUSPlus cDNA vs pDNA: Figure 8A indicates successful cDNA synthesis through amplification of a generic rice housekeeping gene. Primers used for PCR amplification in Figure 8B are specific to GUSPlus transcripts, and bands confirm presence of GUSPlus transcripts only in pDNA-CNT-treated leaf tissues, especially those using a nonbinary vector. Finally, to verify successful pDNA removal by DNase treatment, the PCR of Figure 8C targeted the antibiotic resistance sequence of the GUSPlus vectors. The lack of bands in Figure 8C therefore establishes the absence of residual pDNA in treated samples.

While initial findings seem to indicate CNTs facilitate the passage and expression of pDNA in intact rice leaves and embryos, further investigation is desirable to validate our inferences and interpretations. For instance, NLS-GFP-CNT infiltrations should be repeated, viewing tissues at three days post-treatment rather than waiting four days in unfavorable conditions. Tissue fixing and optical clearing with fluorescent-friendly clearing agents, such as methyl salicylate should also be considered, though fixation and incubation period may decrease fluorescence below levels of detection (Sakhalkar et al., 2007). Finally, in terms of GFP and EYFP transcript analyses, additional control PCRs are necessary to validate successful cDNA syntheses and DNase treatments.

GUSPlus enzymatic activity and transcripts should be evaluated at 24-hour timepoints to verify GUSPlus expression and more extensively delineate its transient nature. Additionally, neither our GUSPlus-specific primers (used in Figure 8B) nor our primers flanking the GUSPlus intron could bind to cDNA from our stably transformed positive control. To properly design and retest primer sets in future experiments, we will require a stably transformed positive control that contains the exact sequence of our GUSPlus cassette. This positive control could be run alongside transcript analyses to validate presence and absence of GUSPlus more convincingly.

Transient expression of reporter plasmids in rice leaves and embryos was evaluated by the expression of fluorescent protein and GUSPlus. Obvious fluorescence and GUSPlus enzymatic activity confirmed pDNA transcription in CNT-treated tissues by both visual imaging and RT-PCR analyses. This evidence validates the CNT ability to transport reporter plasmids across the rice cell wall and nuclear membrane. Binary and nonbinary plasmids both produced visual or transcriptional results indicative of successful expression, demonstrating that DNA cargo can vary in size up to 12.0 kb and still be transported into rice cells when attached to CNTs. Finally, our findings suggest an optimal pDNA-to-CNT ratio around 2:1 for subsequent experiments. We suspect that this ability of CNTs to shuttle pDNA will translate to their use in transporting CRISPR/Cas9 vectors for transient gene editing of rice tissues. Overall, these promising findings with reporter genes support our hypothesis to begin using nanoparticles for *in planta* transformation experiments for gene editing.

3. GENE EDITING BY TRANSIENT EXPRESSION OF CRISPR/CAS VECTORS BY CNT INFILTRATION

3.1. Synopsis

CNTs have been shown to facilitate passive diffusion and transient expression of foreign DNA vectors in intact plant tissues such as leaves. In this chapter, we investigate not only the ability of CNTs to allow diffusion of CRISPR/Cas gene editing vectors into meristematic tissues of rice seeds and mature embryos, but the capacity of these CRISPR cassettes to be transcribed and translated to create gene edits *in planta*. Plasmids expressing CRISPR/Cas9 and single-guide RNAs (sgRNAs) targeting the rice *phytoene desaturase* (*OsPDS*) gene were shown to be expressed and functionally active through the creation of *OsPDS* knockout mutations which were first identified by visual phenotyping before confirmation by gene sequencing.

3.2. Introduction

The global population is expected to increase by nearly two billion by the year 2050 (United Nations, 2015). This increased demand on resources will inevitably strain worldwide food supplies, an outcome which is already exacerbated by decreasing arable land (FAO, 2017). Breakthrough technologies that can expand the food supply are therefore more important than ever to meet the nutritive demands of a steadily growing population. Gene editing technologies offer promise as a tool to mitigate these increasing demands: gene editing can increase yields, nutritive value, and stress tolerance in crops, each improvement helping relieve worldwide malnutrition. In contrast to conventional

breeding methods, gene editing can rapidly create more precise genetic alterations for crop improvement (Scheben et al., 2017; Chen et al., 2019).

While faster crop improvement is essential to win the race against time to feed the population, current gene editing methods are in need of optimization. One of the greatest bottlenecks in plant gene editing is tissue culturing. Circumventing labor-intensive, genotype-specific tissue culture steps of gene editing could expedite development of improved crops while expanding its broader usage.

Here, CNTs loaded with CRISPR/Cas vectors have been shown to induce gene edits in intact rice seeds. This *in planta* technique involves a three-day imbibe in pDNA-CNT solution followed by germination and growth into seedlings, rather than the month-long process necessary for tissue culturing. This *in planta* technique can accelerate the gene editing pipeline by eliminating the need for tissue culturing all together.

3.3. Materials and Methods

3.3.1. Transformation Vectors

CRISPR gene editing plasmids ranged in size from nonbinary vectors just under 9.3 kb to binary vectors nearly 16.2 kb. The two plasmids used most extensively to evaluate gene editing capabilities using CNT transformation included one binary and one nonbinary vector (Table 2).

Table 2 List of Gene Editing Plasmids

Vector Backbone	Reporter Gene	Promoter	Size (kb)
pRGEB32 (binary)	<i>OsPDS</i> sgRNA, Cas9	OsU3, OsUbi	16.2
pTRANS100 (nonbinary)	<i>OsPDS</i> sgRNA, Cas9	OsU3, ZmUbi	9.3

Two sgRNAs (sgRNA1 and sgRNA2) were previously designed to target Exon 4 and Exon 3 of *OsPDS* respectively, and each was verified by *in vitro* assay using cv. Nipponbare and Presidio genomic DNA. Figure 9 depicts exact sgRNA target sites.

```

                                sgRNA2
PDS_Nipponbare_Exon3  AGCTGGTTATCAACCGCAAATATCTGGCAGATGCTGGTCATAAACCCATATTGCTT
PDS_Presidio_Exon3   AGCTGGTTATCAACCGCAAATATCTGGCAGATGCTGGTCATAAACCCATATTGCTT
*****
                                sgRNA1
PDS_Nipponbare_Exon4  ATAGCTGCTTGGAAGGATGAAGATGGAGATGGTATGAAACTGGGCT
PDS_Presidio_Exon4   ATAGCTGCTTGGAAGGATGAAGATGGAGATGGTATGAAACTGGGCT
*****

```

Figure 9. *OsPDS* sgRNAs were designed to target the third and fourth exons of both Nipponbare and Presidio rice genotypes. Target sequences are outlined in red, and the PAM is underlined.

3.3.2. Transient Expression of CRISPR/Cas9 System Targeting *OsPDS*

Mature Nipponbare and Presidio seeds were surface-sterilized and germinated as described in Section 2.3.4. Both excised embryos and full seeds were used in these experiments. Embryos and seeds were mechanically wounded to expose the SAM and subsequently imbibed in a 0.6 M mannitol osmotic solution for at least two hours. Seed tissues were briefly dried on sterile filter paper, then imbibed in a CRISPR/Cas9 pDNA-CNT solution as described previously in Section 2.3.4. Imbibing solutions were concentrated to 1.5 ng/ μ L of plasmid DNA encoding Cas9 and sgRNAs targeting *OsPDS*. Samples were vacuum-infiltrated at 500 mm Hg for up to five minutes and stored at 29 °C on a 14-hour light, 10-hour dark cycle. Select embryos and seeds

were removed from CNT solutions at 24-hour intervals and plated on MS0 agar to form roots and shoots. Plants were grown for at least two weeks to observe possible *OsPDS* knockout phenotypes, which appear as albino and stunted seedlings.

3.3.3. Sanger Sequencing Screening for *OsPDS* Mutations

A quick preliminary screen for *OsPDS* mutations was performed by Sanger sequencing: genomic DNA samples were extracted from pDNA-PEI-CNT treated seedlings using the small-scale CTAB method described by Nekrasov et al., 2017. Genomic DNA was PCR-amplified by primers flanking the *OsPDS* region targeted by our sgRNAs (see Appendix for sequences). PCR products were run on a gel, extracted by Zymoclean Gel DNA Recovery Kit, and ligated into pCR Blunt II-TOPO plasmid vectors as per kit instructions. Plasmids containing the *OsPDS* fragment of interest were cloned into DH5- α *E. coli* (Addgene, 2017), which were then cultured overnight in selective LB liquid medium. DNA was extracted by *Quick*-DNA Miniprep Kit (Zymo Research). Cloned DNA and purified PCR products were sent to either the TAMU Laboratory for Genomic Technology (LGT) or Eurofins for Sanger sequencing using universal or internal primers.

Resulting chromatogram files were initially analyzed by sequence alignment to the original *OsPDS* genomic DNA sequence in Benchling software. Subsequently, Synthego's Inference of CRISPR Edits (ICE) tool was used to batch-analyze .ab1 sequence trace files at each sgRNA site (Hsiao et al., 2018). ICE was able to distinguish multiple sequenced fragments within trace files, allowing quantification and characterization of edits within samples. However, because ICE cannot discern indels

from noise when present at less than 5%, samples that fell below this 5% threshold were discounted (Synthego, 2020). An arbitrary minimum R^2 threshold was chosen at 0.6 to minimize error while still identifying low-frequency mutations.

3.3.4. Confirming *OsPDS* Gene Editing by NGS

Alterations to the *OsPDS* gene of treated seeds and embryos were verified by NGS as follows: genomic DNA samples were extracted from pDNA-PEI-CNT treated seedlings using the small-scale CTAB method described in the previous section. DNA libraries were prepared using Illumina's *16S Metagenomic Sequencing Library Preparation* guide (Illumina, 2013). Primers flanking the sgRNA target sequences are listed in the Appendix. Libraries were sequenced by the TAMU TIGSS facility. Raw sequences were trimmed by FastQC using default settings with a Phred score of 30 (Babraham Bioinformatics) and analyzed using CRIS.py software (Connelly & Pruett-Miller, 2019).

3.4. Results

3.4.1. Visual Analysis of Aberrant Phenotypes

CRISPR/Cas-CNT imbibed seeds and embryos were grown on plant nutrient medium (MS0) for up to two weeks to view alterations in phenotype indicative of *OsPDS* knockout. Seedlings with partially albino leaves and/or stunting were selected for further study (Figure 10).

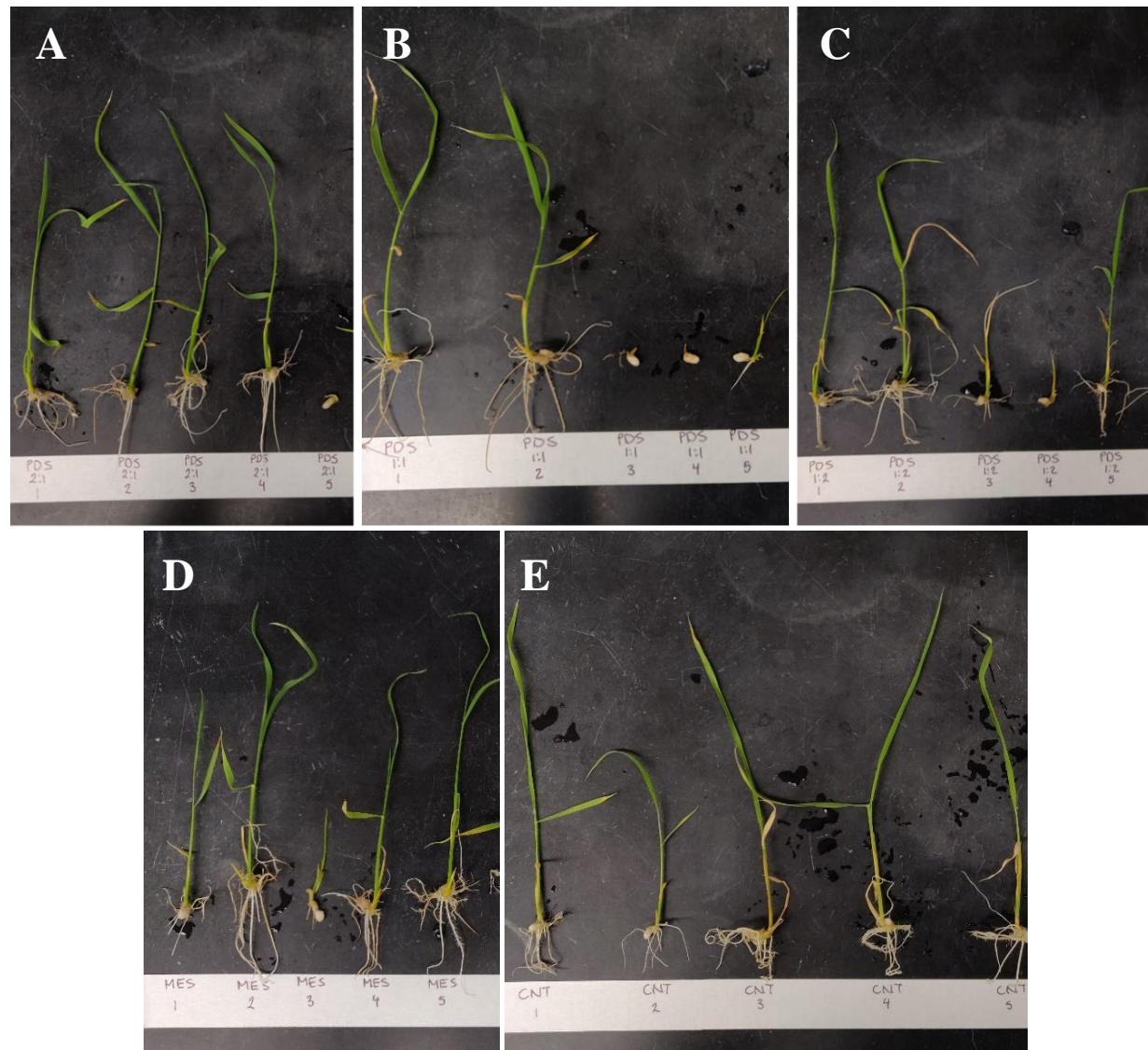


Figure 10. Subset of seeds that were imbibed in pDNA-CNT solutions in 2:1, 1:1, and 1:2 ratios of CRISPR/Cas vectors to CNTs. Seeds were grown on MS0 media plates for up to two weeks. Experimental seeds (**A-C**) that showed altered growth compared to control seeds (**D, E**) were used for subsequent sequencing experiments.

3.4.2. DNA Sequencing of Potential Phenotypic Anomalies

Sanger sequencing of several seedlings with aberrant phenotypes revealed possible mutations and/or poor sequencing quality in the sgRNA target sequences when viewed with the Benchling software (Figure 11).

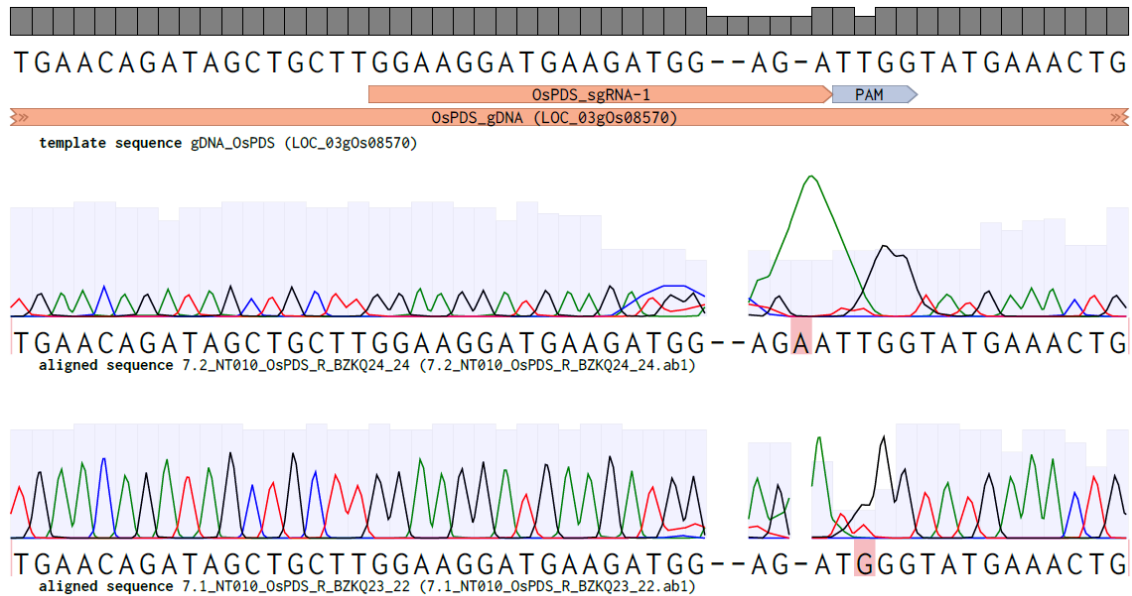


Figure 11. Possible *OsPDS* mutants were cloned, sequenced by Eurofins, and aligned to the wild type *OsPDS* sequence on Benchling.com. The two sequencing chromatograms here show deviations between clones of a single rice sample. Sequences not consistent with the wild type *OsPDS* gene could be indicative of a gene edit.

For more precise analysis of Sanger sequence chromatograms, especially for samples which seemed to contain mixtures of different sequences in the same sample, the Synthego ICE tool was used. The ICE analysis was able to identify a large number of insertion/deletion (INDEL) mutations (Figure 12). A closer inspection of representative ICE alignments for the two *OsPDS* sgRNAs showed the normalized relative contribution of several INDELs: for example, for sgRNA1 a single base pair deletion had a 27%

contribution, the wild type at 26%, and a different base pair deletion 6% (Figure 11A). For sgRNA2, the wild type was 52%, while a single base pair deletion was 9% relative contribution (Figure 11B). Since these sgRNAs are in coding regions, the 1 bp deletions are predicted to cause a frameshift and disrupt the *OsPDS* function, which may lead to the observed stunted phenotypes (Figures 11E and 11F).

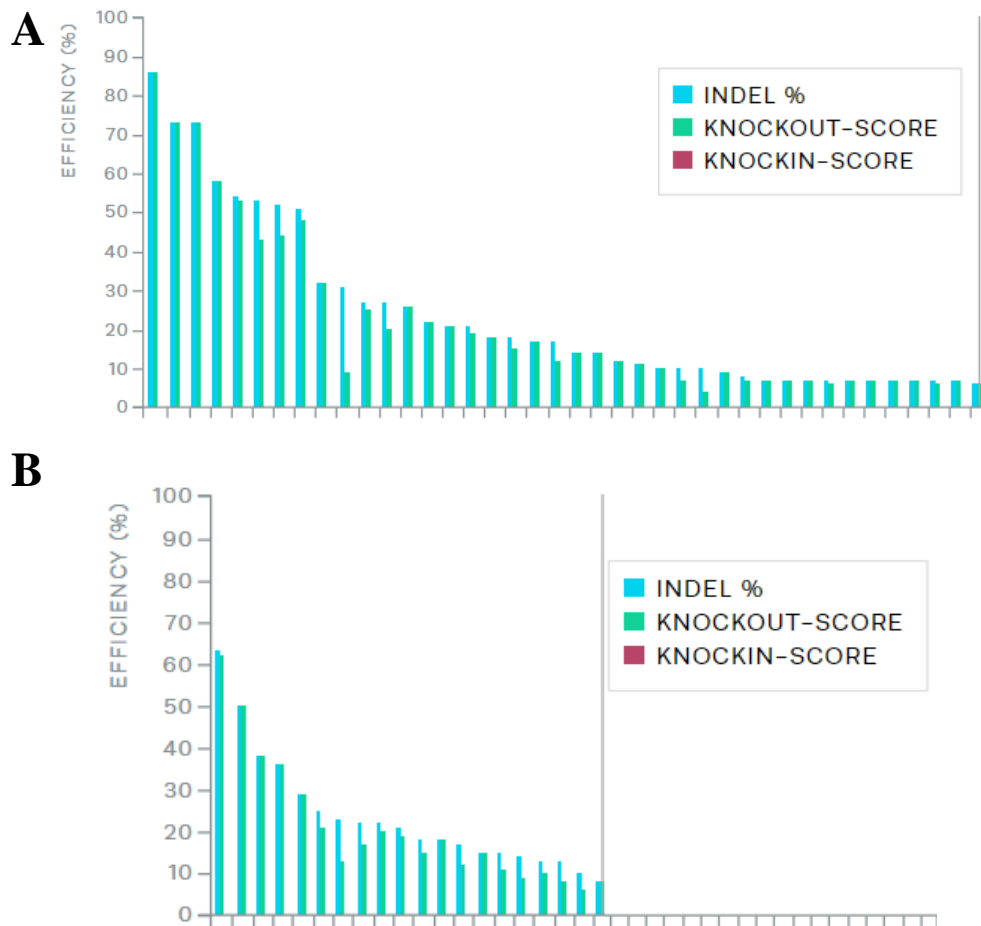


Figure 12. Synthego's ICE analysis of Sanger sequencing results from rice seedlings with possible *OsPDS* knockouts. Analysis was performed separately for sgRNA1 (A) and sgRNA2 (B). Samples with 5% indels or fewer, delineated by vertical grey line, were disregarded. Efficiency is defined as the percent of the sequence pool that deviate from the wild type sequence for each sample. Knockout-score represents the proportion of samples that have either a frameshift or indel greater than 21 bp.

OsPDS Gene Model

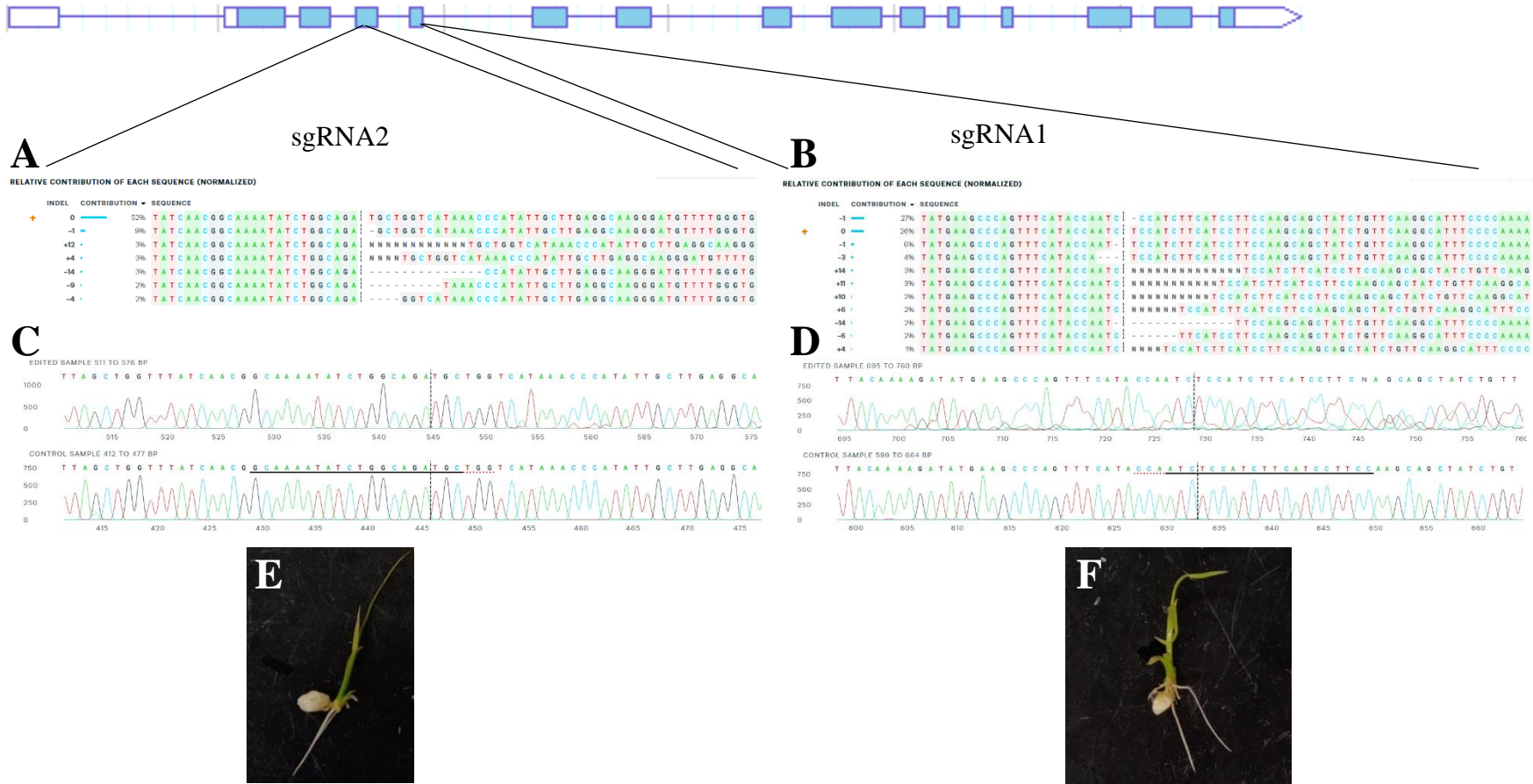


Figure 13. Synthego ICE analysis tool was run on individual trace files returned from Sanger sequencing of potential mutant rice seedlings. **A, B:** sequences present in the edited population and their relative proportions. Expected cut sites (three bp upstream the PAM) are represented by black vertical dotted lines, and the wild type sequence is marked by the orange “+” symbol. **C, D:** Edited vs wild type chromatograms in the region around the guide sequence. Guide sequences are underlined in black, the PAM site is underlined red, and the vertical black dotted line depicts the cut site. **E, F:** aberrant phenotypes of treated seeds that were sent for Sanger sequencing. Overall *OsPDS* gene model from MSU Rice Genome Annotation database.

In contrast to the Sanger sequencing data, a smaller subset of samples that were sequenced using NGS did not reveal INDELS, but instead showed 1% of the sequence reads had a base substitution at the sgRNA2 site after analysis using CRIS.py software (Figure 14).

A

```

Test Sequences:
g2: SCAAAATATCTGGCAGATGCTGG

CGEL-193_S1_L001_R1_val_1.fq TOTAL:201314  Testing: (g2:194715),      Top_reads:[(0, 180098), (1, 15757), (-1, 3816), (2, 1402), (3, 164),
(-2, 56), (4, 15), (5, 3), (6, 3)]
GATAGCAGTCACATCGTGGTCTTAGCATTGTAGTTTTTAGCTTTGATTTTTTTTTTCAGGATTAGCTGGTTTATCAACGGCAAAATATCTGGCAGATGCTGGTCATAAACCCATATTGCTTGAGGCAAGGGATGTTTTGG
GTGG , 166790
GATAGCAGTCACATCGTGGTCTTAGCATTGTAGTTTTTAGCTTTGATTTTTTTTTTCAGGATTAGCTGGTTTATCAACGGCAAAATATCTGGCAGATGCTGGTCATAAACCCATATTGCTTGAGGCAAGGGATGTTTTG
GGTGG , 14459
GATAGCAGTCACATCGTGGTCTTAGCATTGTAGTTTTTAGCTTTGATTTTTTTTTTCAGGATTAGCTGGTTATCAACGGCAAAATATCTGGCAGATGCTGGTCATAAACCCATATTGCTTGAGGCAAGGGATGTTTTGGG
TGG , 3129
GATAGCAGTCACATCGTGGTCTTAGCATTGTAGTTTTTAGCTTTGATTTTTTTTTTCAGGATTAGCTGGTTTATCAACGGCAAAATATCTAGCAGATGCTGGTCATAAACCCATATTGCTTGAGGCAAGGGATGTTTTGG
GTGG , 1950
GATAGCAGTCACATCGTGGTCTTAGCATTGTAGTTTTTAGCTTTGATTTTTTTTTTCAGGATTAGCTGGTTTATCAACGGCAAAATATCTGGCAGATGCTGGTCATAAACCCATATTGCTTGAGGCAAGGGATGTTTT
GGGTGG , 1223
GATAGCAGTCACATCGTGGTCTTAGCATTGTAGTTTTTAGCTTTGATTTTTTTTTTAGGATTAGCTGGTTTATCAACGGCAAAATATCTGGCAGATGCTGGTCATAAACCCATATTGCTTGAGGCAAGGGATGTTTTGG
GTGG , 796
  
```

B

	sgRNA2	
WildType_PDS	TTAGCTGGTTTATCAACG GCAAAATATCTGGCAGATGCTGG TCATAAACCCATATTGCTT	120
CGEL193	TTAGCTGGTTTATCAACGGCAAAATATCT A GCAGATGCTGGTCATAAACCCATATTGCTT	120

Figure 14 A. Trimmed NGS sequence files were analyzed in CRIS.py software for each sgRNA target region to locate mutations in *OsPDS*. Intact, unedited sgRNA target regions are highlighted in yellow. In this sample, 1,950 reads (of 201,314 total) were edited within the sgRNA cut site, a nearly 0.97% editing efficiency. **B.** Aligning the most frequent mutant read to the *OsPDS* wildtype sequence shows a single nucleotide substitution within the sgRNA2 target region of Exon 3. PAM sequence is underlined.

3.5. Discussion

Over the course of this experiment, a total of 1,120 seeds and 112 embryos were imbibed in pDNA-CNT solutions of varying pDNA to CNT ratios. Vectors encoded Cas9 and sgRNAs targeting *OsPDS* for endonuclease activity. All treated seeds and embryos were planted on MS0 plant nutrient media and grown for at least two weeks to evaluate phenotypic differences between treated samples and negative controls. Plants displaying even minute phenotypic differences, such as stunted growth or discolored leaves, were used for subsequent *OsPDS* sequencing validation. We extracted DNA from a total of 121 (10.8%) and 13 (11.6%) phenotypically aberrant seeds and embryos respectively. Though a higher percentage of treated embryos exhibited abnormal phenotypes, labor and time constraints of embryo excision required that we limit the number of samples. Additionally, for unknown reasons, excised embryos did not produce robust plantlets on MS0 agar media like seeds did. These two obstacles presented by embryos forced us to focus on seed treatments.

Sanger sequencing was performed on treated seeds for a quick screen for potential *OsPDS* mutations. Almost 50% of these samples returned with possible variations in at least one of the sgRNA regions, such as in Figure 11. However, much of our Sanger sequencing returned low-quality reads, possibly due to formation of secondary structures or large fragment size (just over 1 kb). Smaller internal primers closer to 0.4 kb were designed as needed to target fragments of *OsPDS* that eluded initial Sanger sequencing. These fragments, unfortunately, still returned with varying degrees

of sequencing quality. Samples that did not return complete, high-quality sequences were then evaluated for mutations by NGS for increased accuracy.

Synthego's ICE tool was used to batch analyze Sanger trace files. This tool could discern individual edited strands within samples, revealing chimeric *OsPDS* knockout samples. Figure 12 shows that out of 103 and 146 high-quality sequencing files covering sgRNA1 and sgRNA2 regions respectively, 43 showed indels in the sgRNA1 target region while only 20 showed indels in the sgRNA2 region. When specifying a minimum R^2 threshold of 0.6, only 33 and 15 samples contained greater than 5% indels in sgRNA1 and sgRNA2 regions respectively. Care must be taken, however, to avoid false positives or sequence analysis artifacts due to low quality sequence data and/or sequencing errors. Figure 13 shows phenotype and mutation information of two such seed samples compared to a wild type control sequence. Figures 13A-D depict multiple mutant sequences within edited samples, as Synthego warns of mixed sequencing bases resulting after the cut due to error-prone repair (ICE.Synthego.com). This information may suggest that chimeric *OsPDS* knockouts have contributed to the stunted, yellowing phenotypes of a subset of treated seedlings. Due to time constraints, not all samples that displayed over 5% indels were analyzed by NGS.

For the smaller subset of samples that were sequenced on an Illumina Miseq, trimmed NGS data analysis using CRIS.py software indicated that there was a single nucleotide substitution within the sgRNA2 target sequence of one seedling sample (Figure 14A). The fourth most frequent read had a single guanine to adenine substitution at position 12 of sgRNA2 (Figure 14B). 1,950 reads out of 201,314 total reads contained

this precise edit, which suggests chimerism at this locus and a nearly 0.97% editing efficiency. Furthermore, this edit is nine base pairs upstream the PAM sequence, which is in the expected seed region for Cas9 endonuclease activity (Wu et al., 2014).

Discrepancies between Illumina results and ICE analyses could have been due to limitations of ICE's predictive capabilities or mutations falling below the 0.95% editing threshold we deemed significant for NGS. Though this single nucleotide substitution was a silent mutation, not affecting the amino acid sequence, overall findings may suggest that CNTs are capable of transforming rice seeds with CRISPR/Cas9 gene editing vectors. Further investigation is necessary to confirm this finding.

Based on the low mutation rates observed, imbibement experiments should be repeated with several adjustments. For instance, infiltrations should be performed on a larger scale: one seed of 1,120 treated showed a high percent of gene editing in the sgRNA target sequence. Treating more seeds and embryos increase our likelihood of producing edited or knockout seedlings. Vacuum infiltration parameters such as time and pressure can be investigated for effects on transformation efficiency. Finally, though sgRNAs were previously validated *in vitro*, new sgRNAs can be designed and tested since binding efficiency could differ *in planta*

Future sequencing strategies should strike a balance between monetary resources, processing time, and reliable results. For instance, NGS could be used to analyze all samples to raise confidence in our sequencing results. These samples could be pooled to offset the increased costs associated with greater NGS processing. Alternatively, future experiments can employ more strict phenotypic screening criteria, such that fewer

samples are processed by Illumina MiSeq but are more likely to contain significant mutations.

Additionally, future experiments should investigate editing efficiency in germline cells and precursors by assessing heritability of edits in progeny. However, *OsPDS* is a suboptimal target for these editing experiments, since knockouts have been shown to induce seed sterility in model plant species (Qin et al., 2007). Alternative target genes involved in pigmentation biosynthesis may still be able to produce viable seed when defunctionalized. For instance, though more research is needed, the *CHLOROPHYLL a OXYGENASE* gene may prove a promising candidate (Lee et al., 2005). Plants with homozygous knockouts could thus display phenotypic deviations yet still allow us to observe gene edits in subsequent generations.

Overall, these experiments reveal possible chimeric gene editing in rice seeds using CNTs to transport CRISPR vectors. While not all phenotypic off-types genotyped were found to contain *pds* alterations, Sanger sequencing and NGS have confirmed at least one plant with detectable sequence changes in the expected sgRNA region. Chimeric mutations seem to indicate that loaded CNTs are capable of traversing the seed coat and inducing CRISPR mechanisms. Protocol optimization could reduce the gene editing pipeline from months to days. The future experiments detailed could potentially evolve this nanotechnology into a straightforward, non-transgenic, *in planta* gene editing system that could bypass the tissue regeneration bottleneck of conventional methods.

4. *IN VITRO* COTTON POLLEN TUBE GROWTH AND CNT INFILTRATION

4.1. Synopsis

CNTs can aid transient plant transformation and may have the capacity to create transgene-free edits in germline cells and their precursors. Efforts have therefore been made to assess CNT ability to induce transient gene editing in cotton (*Gossypium sp.*) pollen tubes. Pollens are germline cells that, if edited, will give rise to edited progeny. Growth of cotton pollen tubes *in vitro* has been documented but not optimized. We aim to improve cotton pollen tube germination systems to enable infiltration of pollen tubes with CNTs. These experiments will help pave the way to a streamlined *in vitro* germline-editing system that generates edited seed and progeny.

4.2. Introduction

Plant tissue culturing, required for *in vitro* transformation and regeneration, is a long, arduous process commonly involved in gene editing. It can take months to regenerate full plants, even for well-studied crops. For instance, it can take up to four months to move maize and rice from transformation to greenhouse planting (Huang and Wei, 2004; Karthikeyan et al., 2009). To complicate matters further, procedures and efficacy of plant regeneration also vary drastically between crops and genotypes.

In contrast, *in planta* transformation methods bypass tissue culturing steps: directly editing germline cells or their precursors assures edits will be inherited in the next generation. Gene edited gametes can directly give rise to gene edited progeny, eliminating the need for *in vitro* regeneration of plants from transformed tissues.

Pollen tubes are outgrowths of germinated pollen grains. Cell wall elongation carries two haploid sperm nuclei down the pistil to fertilize the female gametophyte (Edlund et al., 2004). Creating edits in either pollen or pollen tubes should guarantee heterozygous edits in resulting zygotic progeny. Pollen tubes are likely easier targets for transformation by CNT diffusion as the elongating cell wall is thinner than the protective coat of the pollen grain (Chebli et al., 2012; Ferguson et al., 1998). Previous papers have reported various media preparations that stimulate pollen tube germination *in vitro*, but each protocol reveals limited germination in practice (Burke et al., 2004; Dickinson et al., 2018). In this section, we assess media on which to germinate cotton pollen tubes and apply CNTs.

4.3. Materials and Methods

4.3.1. Cotton Pollen Tube Media Optimization

Cotton pollen germination methods were developed based on those previously published for cotton (*Gossypium hirsutum* and *Gossypium barbadense*) and *Arabidopsis* (Burke et al., 2004; Dickinson et al., 2018). By combining essential components of each paper, we sought to develop a protocol and medium conducive to pollen tube growth across cotton cultivars. Media varying in concentration of key chemicals was poured into Petri plates and cooled to allow the agar to solidify. A layer of cellophane was placed on top of the solid media to emulate the stigmatic surface of a style (Dickinson et al., 2018). Flowers were collected from a variety of cotton cultivars grown in the greenhouse at 30 °C. Pollen grains were immediately dusted onto the cellophane overlaying the media. Petri plates were stored un-capped in plastic containers filled with saturated ammonium

sulfate to maintain 80% humidity (Burke et al., 2004). After three hours incubating in dark conditions at experimental temperatures from 24-29 °C, plates were observed under an Olympus SZX10 stereomicroscope and assessed for pollen tube length and germination efficiency.

4.3.2. Infiltration of Pollen Tubes with CNTs

Once pollen tube growth medium had been optimized and shown to produce consistently efficient germination, pollen tubes were treated with MES delivery buffer (Demirer, Zhang, Goh, et al., 2019) to evaluate their receptibility to transformation by CNT infiltration. As cotton pollen tubes are highly sensitive to excess moisture and humidity (Burke et al., 2004), effects of MES buffer on pollen was first evaluated. Application of 50-100 µL of MES buffer (alkalized to pH 6.7) was examined both before and after pollen germination. Additions of MES concentrated to 10-90% sucrose were also assessed. These aliquots of MES were added at plating or 60 minutes post-plating on germination medium in attempts to create an isotonic solution and limit cell rupturing.

4.4. Results

Initial experiments based on previously published *in vitro* cotton pollen tube media from Burke et al., 2004 did not induce germination in any of our cotton genotypes (Figure 15).



Figure 15. *Gossypium* pollen grains after 5.5 hours on the cotton pollen germination medium of Burke et al. (2004). Pollen grains were incubated at exact pH, humidity, temperature, and media requirements specified, yet no pollen tubes germinated.

Likewise, pollen tube media optimized for *Arabidopsis* from a 2018 Dickinson et al. paper also failed to germinate cotton pollen tubes after over 20 hours on media (Figure 14).

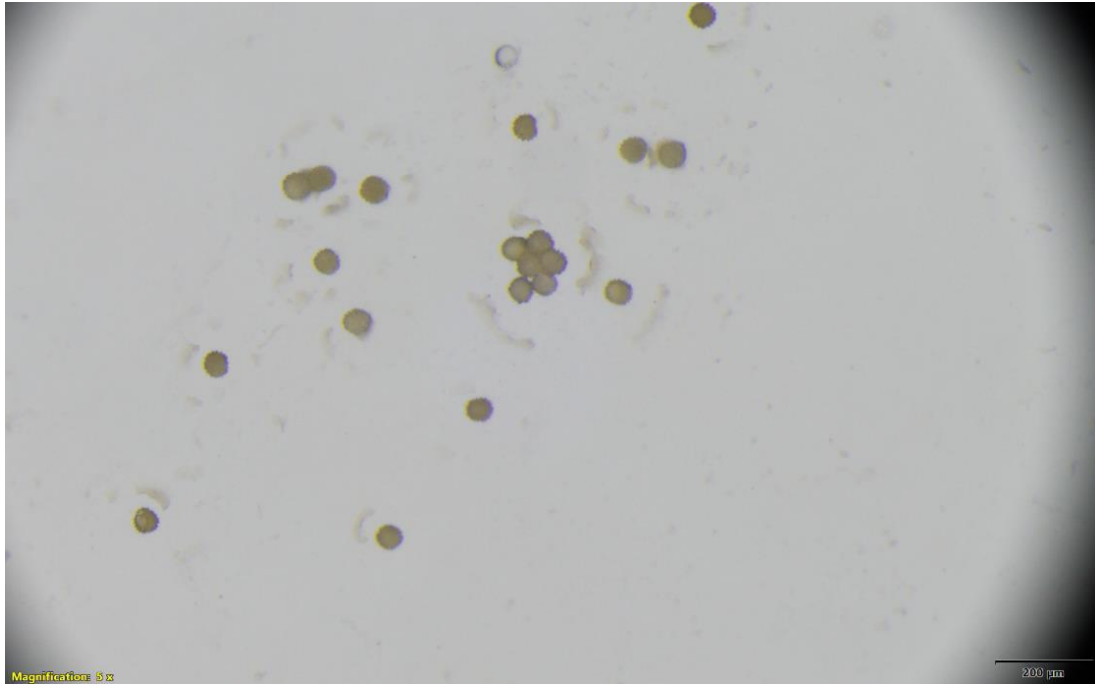


Figure 16. *Gossypium* pollen grains after 20 hours on *Arabidopsis* pollen tube germination medium of Dickinson et al. (2018). Even at optimal temperature and humidity conditions specified for cotton by Burke et al. (2004), no pollen tubes had formed.

Optimization was performed by modifying the concentrations of key components in the media, leading to an improved working media that contained twice the concentration of myo-inositol, spermidine, and GABA when compared to the original Dickinson et al. paper and a 20-fold increase in GA₃ as compared to Burke's 2004 medium. The final working medium yielded sporadic cotton pollen tube germination (Figure 17). Exact

concentrations are as follows: 0.01% (w/v) boric acid, 1 mM calcium chloride, 1 mM calcium nitrate, 1 mM potassium chloride, 0.03% casein enzymatic hydrolysate, 0.01% ferric ammonium citrate, 25%, sucrose, 1% agarose, 0.2 mg/mL myo-inositol, 0.2 mM spermidine, 20 mM GABA, 5 μ M GA₃ (Table 3).

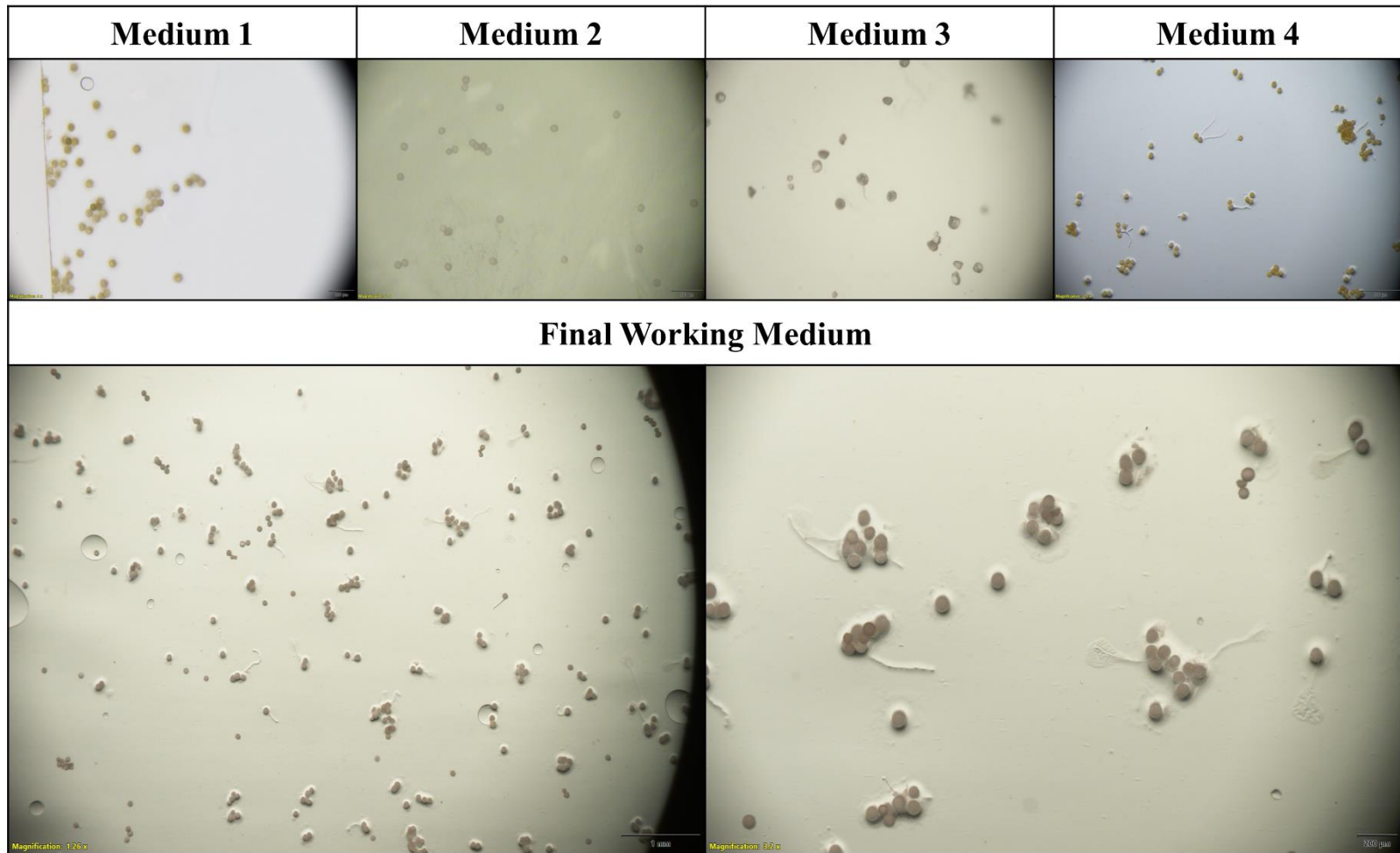


Figure 17. Improvement of pollen tube germination media over a span of several months. Monthly progressions show increased germination frequency and tube length after three-hour incubation. Images depict pollen grains of different *Gossypium* species.

Table 3. Cotton Pollen Germination Media Components and Preparation Methods

Month 1 (Dickinson et al.)	Month 2	Month 3	Month 4	Working Protocol
2mL H ₂ O	1mL H ₂ O	1mL H ₂ O	1mL H ₂ O	1mL H ₂ O
50uL boric acid stock	50uL boric acid stock	50uL boric acid stock	50uL boric acid stock	50uL boric acid stock
100uL calcium chloride stock	100uL calcium chloride stock	100uL calcium chloride stock	100uL calcium chloride stock	100uL calcium chloride stock
100uL calcium nitrate stock	100uL calcium nitrate stock	100uL calcium nitrate stock	100uL calcium nitrate stock	100uL calcium nitrate stock
100uL potassium chloride stock	100uL potassium chloride stock	100uL potassium chloride stock	100uL potassium chloride stock	100uL potassium chloride stock
150uL casein enzymatic hydrolysate stock	150uL casein enzymatic hydrolysate stock	150uL casein enzymatic hydrolysate stock	150uL casein enzymatic hydrolysate stock	150uL casein enzymatic hydrolysate stock
50uL ferric ammonium citrate stock	50uL ferric ammonium citrate stock	50uL ferric ammonium citrate stock	50uL ferric ammonium citrate stock	50uL ferric ammonium citrate stock
0.5g sucrose	50uL GA3 0.1mM solution	10uL myo-inositol stock	Add H ₂ O to bring to ~3.5mL, adjust pH to 7.6	Adjust pH to 7.6
25mg agarose	1.25g sucrose	10uL spermidine stock	1.75g sucrose	1.25g sucrose
MICROWAVE to melt agarose	500mg agarose	100uL GABA stock	50mg agarose	50mg agarose
10uL myo-inositol stock	Bring to 5mL with H ₂ O, adjust pH to 7.6	50uL GA3 0.1mM solution	MICROWAVE to melt agarose	MICROWAVE, allow to cool to 60-65°C in a water bath
10uL spermidine stock	Autoclave to melt agarose	Add H ₂ O to bring to ~3.5mL, adjust pH to 7.6	10uL myo-inositol stock	20uL myo-inositol stock
100uL GABA stock	10uL spermidine stock	1.75g sucrose	10uL spermidine stock	20uL spermidine stock
Bring to 5mL with H ₂ O	10uL spermidine stock	50mg agarose	100uL GABA stock	200uL GABA stock
Adjust pH to 7.0	100uL GABA stock	MICROWAVE to melt agarose	50uL GA3 0.1mM solution	250uL GA3 stock
Pipette onto slides	Pour onto slides	Bring to 5mL with H ₂ O	Bring to 5mL with H ₂ O	Bring to 5mL with H ₂ O
Add cellophane just before use	Add layer of 1.5% agarose just before use	Pipette onto slides	Pipette onto slides	Pour onto mini petri dishes
		Add cellophane just before use	Add cellophane just before use	Add cellophane just before use

In addition, we consistently observed germination frequency between 60% to 67% among all cotton species examined, though pollen tubes varied in length (Figure 18).

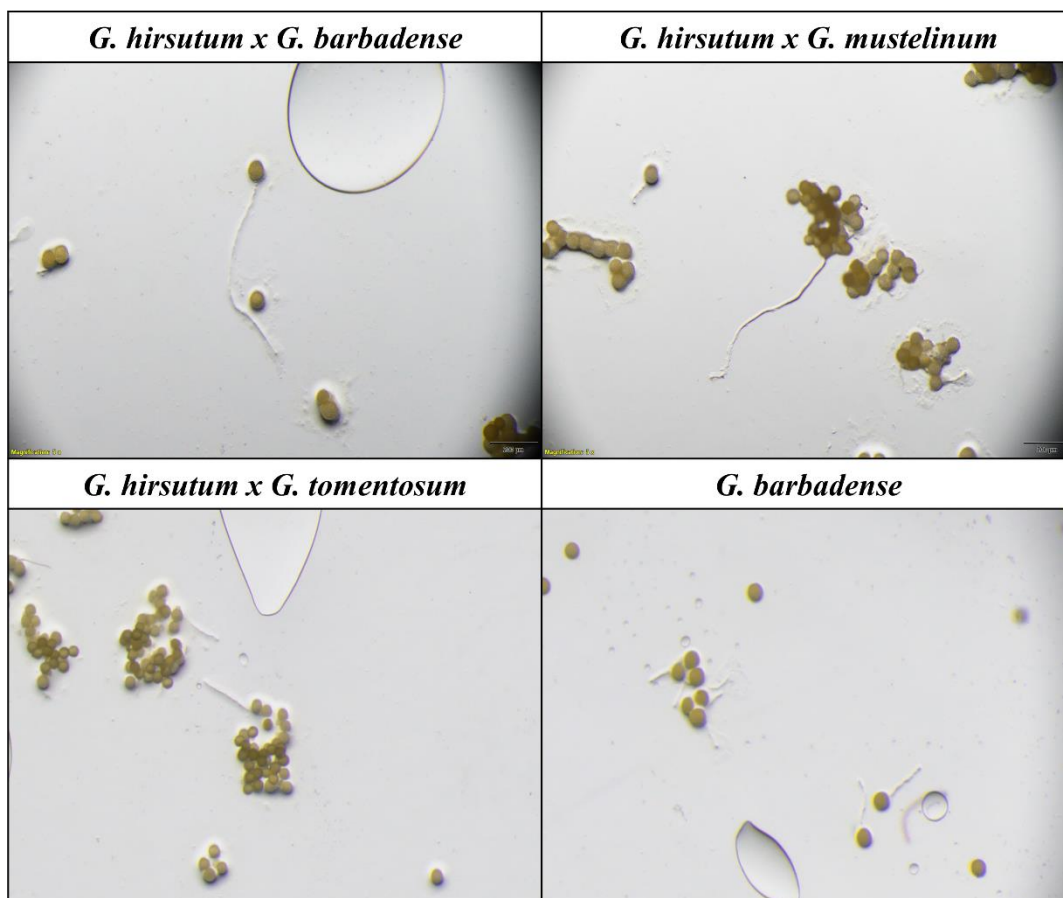


Figure 18. Comparison of pollen tube germination on final working medium between *Gossypium* cultivars. Though pollen tube length differed between genotypes, germination efficiency remained relatively constant.

Once a replicable *in vitro* pollen tube medium had been established, experiments were carried out to assess transformation of pollen tubes with CNTs. Following previously described CNT transformation protocols, we used MES delivery buffer adjusted to pH 6.7. However, adding as little as 50 μ L of MES delivery buffer to pollen before or after pollen tube germination caused cells to rupture within an hour (Figure 19).

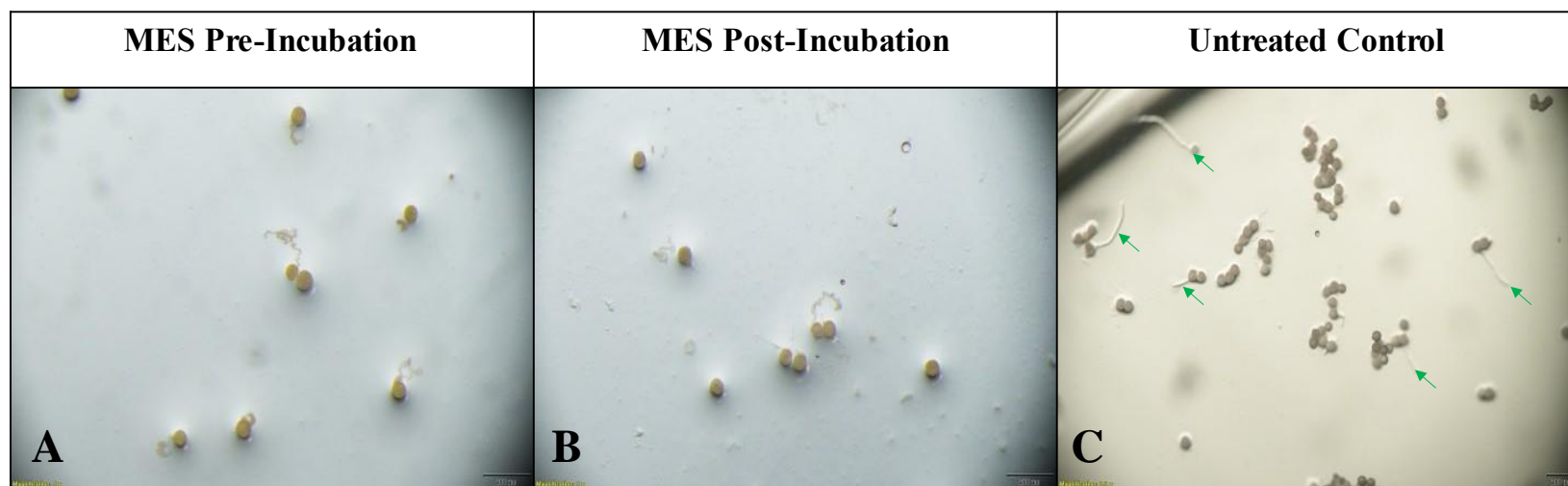


Figure 19. Effect of MES CNT-delivery buffer on pollen grains and pollen tubes. *Gossypium* pollen grains were placed on working germination medium at optimal environmental conditions, and 50 μ L of MES was added to plates either before incubation (**A**) or after a one-hour incubation (**B**). Images were taken two hours after initial plating. Cytoplasmic debris can be seen exuding from pollen grains treated with MES. By comparison, green arrows indicate intact pollen tubes in an untreated control (**C**).

Moreover, cell disruption occurred regardless of sucrose concentration between 10-90% (Figure 20).

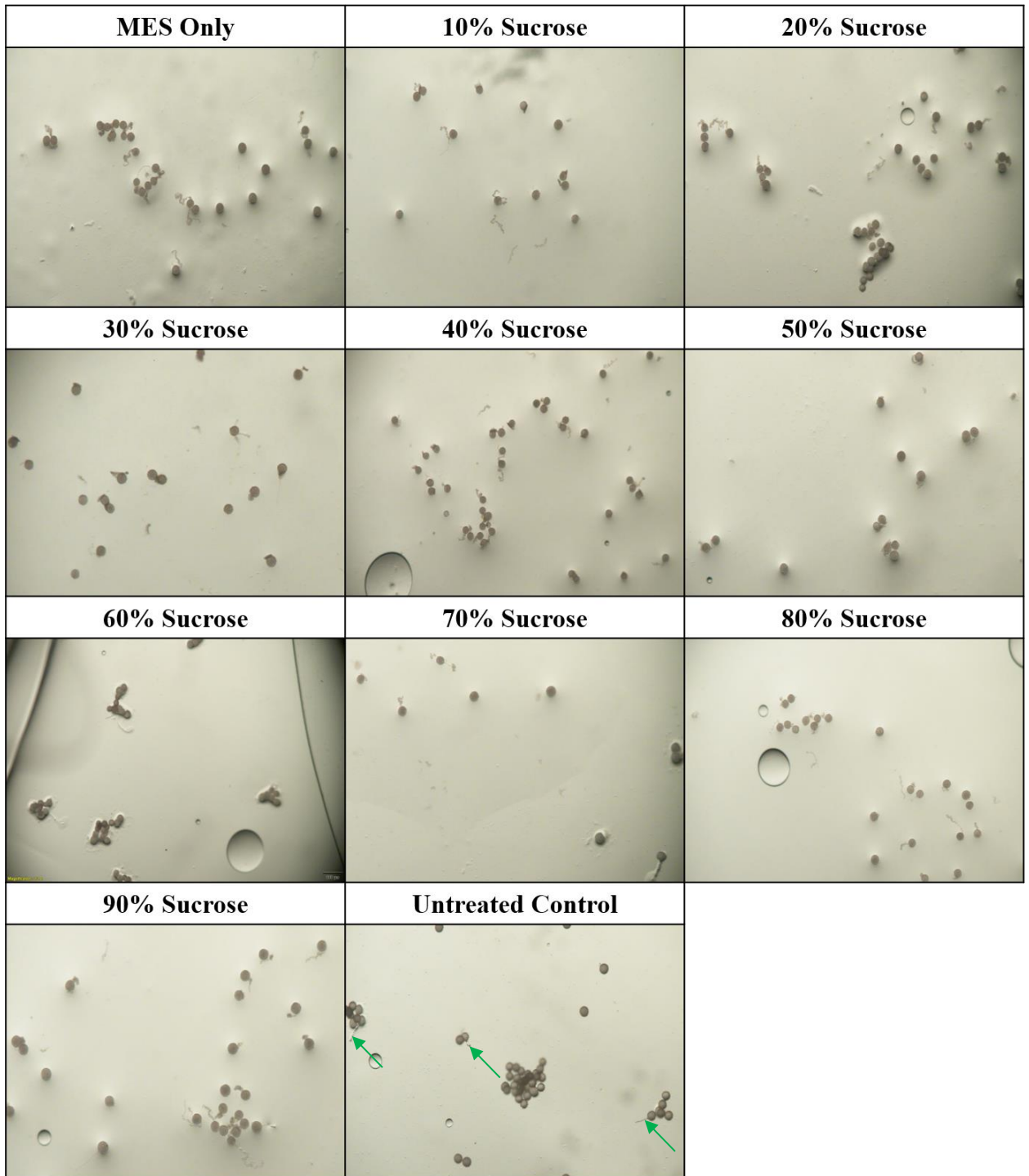


Figure 20. Effect of MES buffer osmolarity on *Gossypium* pollen tubes and pollen grains *in vitro*. Sucrose was dissolved in MES at 10% increments to increase osmolarity and identify isotonic conditions. 50 uL of each solution was added to each plate one hour post-incubation, and images were taken after another one-hour incubation. Cell rupturing was observed in all treated samples. Intact pollen tubes are indicated by green arrows.

4.5. Discussion

Initial experiments replicating the previously published *in vitro* cotton pollen tube media from Burke et al., 2004 did not induce germination in any of our cotton genotypes. The paper specifies that germination should be visible as early as 30 minutes on media. However, Figure 15 shows that even after five hours at the specified temperature and humidity, 100% of pollen grains remained ungerminated. In addition, we replicated pollen tube media optimized for *Arabidopsis* (a model dicot species) from a 2018 Dickinson et al. paper. Cotton pollen was plated on this medium and kept at optimum temperature, humidity, and pH as specified for cotton by Burke et al., 2004. Though Dickinson et al. claim germination should be visible by as early as one hour, pollen tubes had still failed to germinate after over 20 hours on media (Figure 16).

Each component of Dickinson et al.'s *Arabidopsis* pollen germination medium was scrutinized to determine which chemicals were key to increasing germination rates and cell elongation. Research into individual components led us to raise the concentration the key plant metabolites myo-inositol, spermidine, and gamma-aminobutyric acid (GABA), which are known to modulate plant growth, stress tolerance, and possibly even pollen tube growth in model species (Loewus & Loewus, 1983; Mustavi et al., 2018; Renault et al., 2011; Aloisi et al., 2017; Palanivelu et al., 2011). Based on suggestions from Burke et al.'s 2004 protocol, we included A3 gibberellic acid (GA₃), which increases pollen tube germination and elongation. The effects of GA₃ on pollen germination and pollen tube growth have long been known (Bose, 1959). Lastly, we increased the concentration of sucrose in our final working media to create an

isotonic environment and maintain pollen grain integrity. Our final working media, when compared to the original Dickinson et al. paper, contained twice the concentration of myo-inositol, spermidine, and GABA. Additionally, our working media contained a 20-fold increase in GA₃ as compared to Burke's 2004 medium. These four chemicals were found to be essential for pollen tube growth, as elimination of any of these key components inhibited germination (data not shown).

Our experimental design used humidity, temperature, and pH conditions outlined by Burke et al. as they were specifically tailored to cotton. Burke's medium preparation, however, proved more labor-intensive and more difficult to scale-up than that of Dickinson et al. This is mainly due to the 10% agarose content of Burke's medium, which was difficult to dissolve and pour into plates since the agar solidified too quickly. We therefore opted for Dickinson's agarose-cellophane setup instead.

Extensive trial and error of metabolite ratios and incubation conditions led to a final protocol and agarose medium that yielded higher germination rates than previously published protocols. As with previous studies, we found that tubes stopped growing by three hours post-plating on media. Figure 17 depicts a subset of media tested over the span of the optimization process while Table 3 lists media conditions. In addition, we observed germination from pollen of all cotton cultivars tested (Figure 18). Pollen tubes occurred at a relatively constant frequency but varied in length between cultivars. Observed differences could be due to genotypic effects or positional effects in the greenhouse, since pollen viability is affected by growth conditions (Burke et al., 2004; Dickinson et al., 2018; Zhou et al., 2019). Improved germination frequency and

elongation both indicate high cell activity and provide more surface area over which to infiltrate with CNTs in future experiments.

Once a medium was established for replicable *in vitro* pollen germination and pollen tube growth, experiments were carried out to assess transformation of pollen tubes with CNTs. Following previously described CNT transformation protocols, we used MES delivery buffer (25 mM MES, 15 mM MgCl₂, pH 6.0) as the liquid medium in which to deliver nanotubes. However, cotton pollen grains are highly sensitive to humidity, and contact with liquid causes them to rupture. To prevent osmotic pressure from rupturing pollen, the osmolarity of MES delivery buffer was increased to create an isotonic environment. Sucrose was added in incremental volumes to MES delivery buffer, fully dissolved, and added at different time points during *in vitro* pollen tube development. Adding as little as 50 μ L of 80 Osm MES delivery buffer to pollen before or after pollen tube germination caused cells to rupture (Figure 19). Moreover, cell disruption occurred regardless of sucrose concentration between 10-90% (Figure 20). The null response of pollen to changes in osmolarity suggest the pH or composition of MES buffer per se is problematic. For instance, concentration of MgCl₂ has been shown to have variable effects on pollen tube germination in other plant species (Reddy & Goss, 1971; Yokota et al., 2004). Regardless, ruptured pollen tubes would be unusable for downstream gene editing and fertilization. These findings indicate that current MES delivery buffer is unsuitable for transforming cotton pollen tubes with CNTs. Further research must be conducted to determine an optimal delivery buffer, one that proves innocuous to both pollen and PEI-CNTs.

Overall, we have developed a solid agarose medium capable of inducing highly efficient *in vitro* pollen tube germination across *Gossypium* genotypes. Our medium has improved upon previous studies by increasing concentrations of myo-inositol, spermidine, GABA and GA₃. Attempts to transform cotton pollen tubes have been hindered by our inability to add MES delivery buffer to pollen *in vitro* without damaging our biological material. The observed reaction of cotton pollen to the MES buffer indicates an alternative CNT-delivery medium will be needed, i.e., one that neither disrupts pollen cells nor negatively affects CRISPR/Cas9-CNTs. Alternative CRISPR delivery methods such as particle bombardment may also be investigated. If pollen tubes are successfully transfected, future efforts can be taken screen for gene-edited sperm nuclei to initiate fertilization, thereby establishing a tissue-culture-free gene editing system.

5. CONCLUSIONS

Genome editing is essential for adapting crops to modern-day demands. However, current methods entail bottlenecks such as tissue culturing and plant regeneration. This project aimed to eliminate tissue culturing all together by taking advantage of nanoparticles, specifically carbon nanotubes (CNTs). CNTs are non-toxic to biological systems at low concentrations, are capable of electrostatically attaching to DNA, and fall below cell wall and cell membrane size exclusion limits. CNTs did in fact prove valuable as their passive diffusion across cell walls and membranes offered a genotype-independent mechanism to transport CRISPR vectors for *in planta* gene editing.

We found that CNTs are capable of traversing plant cell walls to deliver reporter plasmids in intact rice tissues. Evidence was obtained from two reporter systems—fluorescent proteins and GUSPlus proteins—both expressed *in planta* after pDNA-CNT imbibement. CNTs were able to transport plasmids ranging from 3.7 kb to 12.0 kb in size. Transcription was validated by cDNA analysis to confirm visual indicators.

CNTs were also shown deliver CRISPR/Cas9 gene editing vectors across the seed coat. Sanger sequencing and NGS both suggest that plasmids grafted to CNTs were transcribed and able to induce gene edits in seeds. Though further experimentation and assay modifications are necessary to increase editing efficiency, CNTs show promise as a mode for *in planta* gene editing.

Modifications to previously published pollen tube germination media led to medium for replicable albeit sporadic cotton pollen germination and pollen tube growth. Working protocols now function across several tested *Gossypium* genotypes with greater efficiency than could be reproduced on previously reported media. MES CNT-delivery buffer was highly detrimental to cotton pollen and pollen tubes.

6. REFERENCES

- Addgene Protocol—Bacterial Transformation*. (November 13, 2017). Addgene.
<https://www.addgene.org/protocols/bacterial-transformation/>
- Aloisi, I., Cai, G., Faleri, C., Navazio, L., Serafini-Fracassini, D., & Del Duca, S. (2017). Spermine Regulates Pollen Tube Growth by Modulating Ca²⁺-Dependent Actin Organization and Cell Wall Structure. *Frontiers in Plant Science*, 8.
<https://doi.org/10.3389/fpls.2017.01701>
- Altpeter, Fredy, Nathan M. Springer, Laura E. Bartley, Ann E. Blechl, Thomas P. Brutnell, Vitaly Citovsky, Liza J. Conrad, et al. “Advancing Crop Transformation in the Era of Genome Editing.” *The Plant Cell* 28, no. 7 (July 1, 2016): 1510–20.
<https://doi.org/10.1105/tpc.16.00196>
- Anbu, P. & Arul, Loganathan. (2013). Beta glucuronidase activity in early stages of rice seedlings and callus: A comparison with *Escherichia coli* beta glucuronidase expressed in the transgenic rice. *International Journal of Biotechnology and Molecular Biology Research*, 4(4), 52–59. <https://doi.org/10.5897/IJBMBR2013.0152>
- Andrieu, A., Breitler, J. C., Siré, C., Meynard, D., Gantet, P., & Guiderdoni, E. (2012). An in planta, *Agrobacterium*-mediated transient gene expression method for inducing gene silencing in rice (*Oryza sativa* L.) leaves. *Rice*, 5(1), 23. <https://doi.org/10.1186/1939-8433-5-23>
- Banakar, R., & Wang, K. (2020). Biolistic Transformation of Japonica Rice Varieties. In S. Rustgi & H. Luo (Eds.), *Biolistic DNA Delivery in Plants: Methods and Protocols* (pp. 163–176). Springer US. https://doi.org/10.1007/978-1-0716-0356-7_8
- Barrangou, R., Fremaux, C., Deveau, H., Richards, M., Boyaval, P., Moineau, S., Romero, D. A., & Horvath, P. (2007). CRISPR Provides Acquired Resistance Against Viruses in Prokaryotes. *Science*, 315(5819), 1709–1712. <https://doi.org/10.1126/science.1138140>
- Bose, N. (1959). Effect of Gibberellin on the Growth of Pollen Tubes. *Nature*, 184(4698), 1577–1577. <https://doi.org/10.1038/1841577a0>
- Brouns, Stan, Matthijs Jore, Magnus Lundgren, Edze Westra, Rik Slijkhuis, Bram Snijders, Mark Dickman, Kira Makarova, Eugene Koonin, and John Oost. “Small CRISPR RNAs Guide Antiviral Defense in Prokaryotes.” *Science* (New York, N.Y.) 321 (September 1, 2008): 960–64. <https://doi.org/10.1126/science.1159689>

- Burke, John J., Jeff Velten, and Melvin J. Oliver. “In Vitro Analysis of Cotton Pollen Germination.” *Agronomy Journal* 96, no. 2 (2004): 359–68.
<https://doi.org/10.2134/agronj2004.3590>
- Cervera, M. (2004). Histochemical and Fluorometric Assays for uidA (GUS) Gene Detection. In L. Peña (Ed.), *Transgenic Plants: Methods and Protocols* (pp. 203–213). Humana Press. <https://doi.org/10.1385/1-59259-827-7:203>
- Chebli, Y., Kaneda, M., Zerzour, R., & Geitmann, A. (2012). The Cell Wall of the Arabidopsis Pollen Tube—Spatial Distribution, Recycling, and Network Formation of Polysaccharides1[C][W][OA]. *Plant Physiology*, 160(4), 1940–1955.
<https://doi.org/10.1104/pp.112.199729>
- Chen, K., Wang, Y., Zhang, R., Zhang, H., & Gao, C. (2019). CRISPR/Cas Genome Editing and Precision Plant Breeding in Agriculture. *Annual Review of Plant Biology*, 70(1), 667–697. <https://doi.org/10.1146/annurev-arplant-050718-100049>
- Chen, Q. & Lai, H. (2015). Gene delivery into plant cells for recombinant protein production. *Biomed. Res. Int.* 932161. <https://doi.org/10.1155/2015/932161>
- Connelly, J. P., & Pruett-Miller, S. M. (2019). CRIS.py: A Versatile and High-throughput Analysis Program for CRISPR-based Genome Editing. *Scientific Reports*, 9(1), 4194. <https://doi.org/10.1038/s41598-019-40896-w>
- Dickinson, Hugh, Josefina Rodriguez-Enriquez, and Robert Grant-Downton. “Pollen Germination and Pollen Tube Growth of Arabidopsis Thaliana: In Vitro and Semi in Vivo Methods.” *BIO-PROTOCOL* 8, no. 16 (2018).
<https://doi.org/10.21769/BioProtoc.2977>
- Decaestecker, W., Buono, R. A., Pfeiffer, M. L., Vangheluwe, N., Jourquin, J., Karimi, M., Isterdael, G. V., Beeckman, T., Nowack, M. K., & Jacobs, T. B. (2019). CRISPR-TSKO: A Technique for Efficient Mutagenesis in Specific Cell Types, Tissues, or Organs in Arabidopsis. *The Plant Cell*, 31(12), 2868–2887.
<https://doi.org/10.1105/tpc.19.00454>
- Demirer, G. S., Zhang, H., Goh, N. S., González-Grandío, E., & Landry, M. P. (2019). Carbon nanotube-mediated DNA delivery without transgene integration in intact plants. *Nature Protocols*, 14(10), 2954–2971. <https://doi.org/10.1038/s41596-019-0208-9>
- Demirer, G. S., Zhang, H., Matos, J. L., Goh, N. S., Cunningham, F. J., Sung, Y., Chang, R., Aditham, A. J., Chio, L., Cho, M.-J., Staskawicz, B., & Landry, M. P. (2019). High aspect ratio nanomaterials enable delivery of functional genetic material without DNA integration in mature plants. *Nature Nanotechnology*, 14(5), 456–464.
<https://doi.org/10.1038/s41565-019-0382-5>

- Dutt, M., Li, Z. T., Dhekney, S. A., & Gray, D. J. (2007). Transgenic plants from shoot apical meristems of *Vitis vinifera* L. “Thompson Seedless” via *Agrobacterium*-mediated transformation. *Plant Cell Reports*, *26*(12), 2101–2110. <https://doi.org/10.1007/s00299-007-0424-6>
- Edlund, A. F., Swanson, R., & Preuss, D. (2004). Pollen and stigma structure and function: The role of diversity in pollination. *The Plant Cell*, *16*(Suppl), S84–S97. <https://doi.org/10.1105/tpc.015800>
- FAO (2017). The future of food and agriculture: Trends and challenges (FAO).
- Ferguson, C., Teeri, T. T., Siika-aho, M., Read, S. M., & Bacic, A. (1998). Location of cellulose and callose in pollen tubes and grains of *Nicotiana tabacum*. *Planta*, *206*(3), 452–460. <https://doi.org/10.1007/s004250050421>
- Himmel, M. E., Ding, S.-Y., Johnson, D. K., Adney, W. S., Nimlos, M. R., Brady, J. W., & Foust, T. D. (2007). Biomass Recalcitrance: Engineering Plants and Enzymes for Biofuels Production. *Science*, *315*(5813), 804–807. <https://doi.org/10.1126/science.1137016>
- Hsiau, T., Maures, T., Waite, K., Yang, J., Kelso, R., Holden, K., & Stoner, R. (2018). *Inference of CRISPR Edits from Sanger Trace Data* (p. 251082). <https://doi.org/10.1101/251082>
- Huang, X.-Q., & Wei, Z.-M. (2004). High-frequency plant regeneration through callus initiation from mature embryos of maize (*Zea Mays* L.). *Plant Cell Reports*, *22*(11), 793–800. <https://doi.org/10.1007/s00299-003-0748-9>
- Hwang, H.-H., Yu, M., & Lai, E.-M. (2017). *Agrobacterium*-mediated plant transformation: Biology and applications. *The Arabidopsis Book*, *15*. <https://doi.org/10.1199/tab.0186>
- Synthego’s ICE Tool Limitations. (2020). Synthego. <https://www.synthego.com/help/ice-limitations>
- Illumina. (2013). *16S Metagenomic Sequencing Library* (Rev. B). Retrieved from https://support.illumina.com/content/dam/illumina-support/documents/documentation/chemistry_documentation/16s/16s-metagenomic-library-prep-guide-15044223-b.pdf
- Jinek, Martin, Krzysztof Chylinski, Ines Fonfara, Michael Hauer, Jennifer Doudna, and Emmanuelle Charpentier. “A Programmable Dual-RNA-Guided DNA Endonuclease in Adaptive Bacterial Immunity.” *Science* (New York, N.Y.) *337* (June 28, 2012): 816–21. <https://doi.org/10.1126/science.1225829>

- Karthikeyan, A., Pandian, S. T. K., & Ramesh, M. (2009). High frequency plant regeneration from embryogenic callus of a popular indica rice (*Oryza sativa* L.). *Physiology and Molecular Biology of Plants : An International Journal of Functional Plant Biology*, 15(4), 371–375. <https://doi.org/10.1007/s12298-009-0042-6>
- Kawahara, Y., de la Bastide, M., Hamilton, J.P. *et al.* (2013). Improvement of the *Oryza sativa* Nipponbare reference genome using next generation sequence and optical map data. *Rice* 6, 4. <https://doi.org/10.1186/1939-8433-6-4>
- Krichevsky, A., Kozlovsky, S. V., Tian, G.-W., Chen, M.-H., Zaltsman, A., & Citovsky, V. (2007). How pollen tubes grow. *Developmental Biology*, 303(2), 405–420. <https://doi.org/10.1016/j.ydbio.2006.12.003>
- Kungulovski, G., & Jeltsch, A. (2016). Epigenome Editing: State of the Art, Concepts, and Perspectives. *Trends in Genetics*, 32(2), 101–113. <https://doi.org/10.1016/j.tig.2015.12.001>
- Ledford, H. (2019). Super-precise new CRISPR tool could tackle a plethora of genetic diseases. *Nature*, 574(7779), 464–465. <https://doi.org/10.1038/d41586-019-03164-5>
- Lee, S., Kim, J.-H., Yoo, E. S., Lee, C.-H., Hirochika, H., & An, G. (2005). Differential regulation of chlorophyll a oxygenase genes in rice. *Plant Molecular Biology*, 57(6), 805–818. <https://doi.org/10.1007/s11103-005-2066-9>
- Lew, T. T. S., Park, M., Wang, Y., Gordiichuk, P., Yeap, W.-C., Mohd Rais, S. K., Kulaveerasingham, H., & Strano, M. S. (2020). Nanocarriers for Transgene Expression in Pollen as a Plant Biotechnology Tool. *ACS Materials Letters*, 1057–1066. <https://doi.org/10.1021/acsmaterialslett.0c00247>
- Liu, J., Nannas, N. J., Fu, F., Shi, J., Aspinwall, B., Parrott, W. A., & Dawe, R. K. (2019). Genome-Scale Sequence Disruption Following Biolistic Transformation in Rice and Maize. *The Plant Cell*, 31(2), 368. <https://doi.org/10.1105/tpc.18.00613>
- Loewus, F. A., & Loewus, M. W. (1983). myo-Inositol: Its Biosynthesis and Metabolism. *Annual Review of Plant Physiology*, 34(1), 137–161. <https://doi.org/10.1146/annurev.pp.34.060183.001033>
- Makarova, K. S., Aravind, L., Wolf, Y. I., & Koonin, E. V. (2011). Unification of Cas protein families and a simple scenario for the origin and evolution of CRISPR-Cas systems. *Biology Direct*, 6(1), 38. <https://doi.org/10.1186/1745-6150-6-38>
- Makarova, Kira S., Yuri I. Wolf, Omer S. Alkhnbashi, Fabrizio Costa, Shiraz A. Shah, Sita J. Saunders, Rodolphe Barrangou, et al. “An Updated Evolutionary Classification of

- CRISPR–Cas Systems.” *Nature Reviews Microbiology* 13, no. 11 (November 2015): 722–36. <https://doi.org/10.1038/nrmicro3569>
- Marzec, M., Braszewska-Zalewska, A., & Hensel, G. (2020). Prime Editing: A New Way for Genome Editing. *Trends in Cell Biology*, 30(4), 257–259. <https://doi.org/10.1016/j.tcb.2020.01.004>
- Mustafavi, S. H., Naghdi Badi, H., Şekara, A., Mehrafarin, A., Janda, T., Ghorbanpour, M., & Rafiee, H. (2018). Polyamines and their possible mechanisms involved in plant physiological processes and elicitation of secondary metabolites. *Acta Physiologiae Plantarum*, 40(6), 102. <https://doi.org/10.1007/s11738-018-2671-2>
- Nekrasov, V., Wang, C., Win, J., Lanz, C., Weigel, D., & Kamoun, S. (2017). Rapid generation of a transgene-free powdery mildew resistant tomato by genome deletion. *Scientific Reports*, 7(1), 482. <https://doi.org/10.1038/s41598-017-00578-x>
- Palanivelu, R., Brass, L., Edlund, A. F., & Preuss, D. (2003). Pollen Tube Growth and Guidance Is Regulated by POP2, an Arabidopsis Gene that Controls GABA Levels. *Cell*, 114(1), 47–59. [https://doi.org/10.1016/S0092-8674\(03\)00479-3](https://doi.org/10.1016/S0092-8674(03)00479-3)
- Qin, Genji, Hongya Gu, Ligeng Ma, Yiben Peng, Xing Wang Deng, Zhangliang Chen, and Li-Jia Qu. “Disruption of Phytoene Desaturase Gene Results in Albino and Dwarf Phenotypes in Arabidopsis by Impairing Chlorophyll, Carotenoid, and Gibberellin Biosynthesis.” *Cell Research* 17, no. 5 (May 2007): 471–82. <https://doi.org/10.1038/cr.2007.40>
- Reddy, P. R., & Goss, J. A. (1971). Effect of Salinity on Pollen. I. Pollen Viability as Altered by Increasing Osmotic Pressure with NaCl, MgCl₂, and CaCl₂. *American Journal of Botany*, 58(8), 721–725. <https://doi.org/10.2307/2441469>
- Renault, H., El Amrani, A., Palanivelu, R., Updegraff, E. P., Yu, A., Renou, J.-P., Preuss, D., Bouchereau, A., & Deleu, C. (2011). GABA Accumulation Causes Cell Elongation Defects and a Decrease in Expression of Genes Encoding Secreted and Cell Wall-Related Proteins in Arabidopsis thaliana. *Plant and Cell Physiology*, 52(5), 894–908. <https://doi.org/10.1093/pcp/pcr041>
- Sakhalkar, H. S., Dewhirst, M., Oliver, T., Cao, Y., & Oldham, M. (2007). Functional imaging in bulk tissue specimens using optical emission tomography: Fluorescence preservation during optical clearing. *Physics in Medicine and Biology*, 52(8), 2035–2054. <https://doi.org/10.1088/0031-9155/52/8/001>
- Sander, J. D., & Joung, J. K. (2014). CRISPR-Cas systems for editing, regulating and targeting genomes. *Nature Biotechnology*, 32(4), 347–355. <https://doi.org/10.1038/nbt.2842>

- Sato, S., Newell, C., Kolacz, K., Tredo, L., Finer, J., & Hinchee, M. (1993). Stable transformation via particle bombardment in two different soybean regeneration systems. *Plant Cell Reports*, *12*(7), 408–413. <https://doi.org/10.1007/BF00234702>
- Scheben, A., Wolter, F., Batley, J., Puchta, H., & Edwards, D. (2017). Towards CRISPR/Cas crops – bringing together genomics and genome editing. *New Phytologist*, *216*(3), 682–698. <https://doi.org/10.1111/nph.14702>
- Smith, P. J., Wiltshire, M., & Errington, R. J. (2004). DRAQ5 Labeling of Nuclear DNA in Live and Fixed Cells. *Current Protocols in Cytometry*, *28*(1), 7.25.1-7.25.11. <https://doi.org/10.1002/0471142956.cy0725s28>
- Tamura, K., Shimada, T., Ono, E., Tanaka, Y., Nagatani, A., Higashi, S., Watanabe, M., Nishimura, M., & Hara-Nishimura, I. (2003). Why green fluorescent fusion proteins have not been observed in the vacuoles of higher plants. *The Plant Journal*, *35*(4), 545–555. <https://doi.org/10.1046/j.1365-313X.2003.01822.x>
- Turnbull, C., Lillemo, M., & Hvoslef-Eide, T. A. K. (2021). Global Regulation of Genetically Modified Crops Amid the Gene Edited Crop Boom – A Review. *Frontiers in Plant Science*, *12*, 258. <https://doi.org/10.3389/fpls.2021.630396>
- UniProt: A worldwide hub of protein knowledge. (2019). *Nucleic Acids Research*, *47*(D1), D506–D515. <https://doi.org/10.1093/nar/gky1049>
- United Nations. (2015). *World Population Prospects: The 2015 Revision, Key Findings and Advance Tables*. Retrieved from https://population.un.org/wpp/Publications/Files/Key_Findings_WPP_2015.pdf
- UMBC. (n.d.). *Determining Fluorescence Intensity and Signal*. Keith R. Porter Imaging Facility. Retrieved May 21, 2021, from <https://kpif.umbc.edu/image-processing-resources/imagej-fiji/determining-fluorescence-intensity-and-positive-signal/>
- Wang, M., Sun, R., Zhang, B., & Wang, Q. (2019). Pollen Tube Pathway-Mediated Cotton Transformation. In B. Zhang (Ed.), *Transgenic Cotton: Methods and Protocols* (pp. 67–73). Springer. https://doi.org/10.1007/978-1-4939-8952-2_6
- Wardrop, J., Lowe, K. C., Power, J. B., & Davey, M. R. (1996). Perfluorochemicals and plant biotechnology: An improved protocol for protoplast culture and plant regeneration in rice (*Oryza sativa* L.). *Journal of Biotechnology*, *50*(1), 47–54. [https://doi.org/10.1016/0168-1656\(96\)01548-9](https://doi.org/10.1016/0168-1656(96)01548-9)
- Wu, X., Kriz, A. J., & Sharp, P. A. (2014). Target specificity of the CRISPR-Cas9 system. *Quantitative Biology*, *2*(2), 59–70. <https://doi.org/10.1007/s40484-014-0030-x>

- Xu, R., Qin, R., Li, H., Li, D., Li, L., Wei, P., & Yang, J. (2017). Generation of targeted mutant rice using a CRISPR-Cpf1 system. *Plant Biotechnology Journal*, *15*(6), 713–717. <https://doi.org/10.1111/pbi.12669>
- Yang, L., Cui, G., Wang, Y., Hao, Y., Du, J., Zhang, H., Wang, C., Zhang, H., Wu, S.-B., & Sun, Y. (2017). Expression of Foreign Genes Demonstrates the Effectiveness of Pollen-Mediated Transformation in *Zea mays*. *Frontiers in Plant Science*, *8*. <https://doi.org/10.3389/fpls.2017.00383>
- Yokota, E., Ohmori, T., Muto, S., & Shimmen, T. (2004). 21-kDa polypeptide, a low-molecular-weight cyclophilin, is released from pollen of higher plants into the extracellular medium in vitro. *Planta*, *218*(6), 1008–1018. <https://doi.org/10.1007/s00425-003-1177-2>
- Zhang, Y., Yin, X., Yang, A., Li, G., & Zhang, J. (2005). Stability of inheritance of transgenes in maize (*Zea mays* L.) lines produced using different transformation methods. *Euphytica*, *144*(1–2), 11–22. <https://doi.org/10.1007/s10681-005-4560-1>
- Zhou, H., Hu, Q., Zhang, C., Hu, S., Chen, Q., & Tang, C. (2019). High Temperature Reduces the Viability of Pollen from Upland Cotton in China. *Agronomy Journal*, *111*(6), 3039–3047. <https://doi.org/10.2134/agronj2019.03.0150>

APPENDIX

SUPPLEMENTAL FIGURES AND TABLES

Table 4 Primers used for PCR amplification. Primer sets used for Illumina NGS library adapter PCR do not include adapter sequences.

Primer Code	Target	Sequence (5' to 3')
NT068	GFP transcripts (F)	TGAGGGATACGTGCAGGAG
NT069	GFP transcripts (R)	TGCCGTTCTTTTGCTTGTCG
NT076	YFP transcripts (R)	AAGAAGATGGTGCCTCCTG
NT077	YFP transcripts (F)	ACGTAAACGGCCACAAGTTC
NT122	Elongation Factor 1- α (F)	TCATCATGAACCACCCTGGC
NT123	Elongation Factor 1- α (R)	TGGGCTTGGTGGGAATCATC
NT035	HPT (F)	TCCGACCTGATGCAGCTCTC
NT036	HPT (R)	GATTCCTTGCAGTCCGAATG
NT039	GUSPlus transcripts (F)	GCACCATCAAGACGTTCTCC
NT040	GUSPlus transcripts (R)	CTTCTGTGGGTCGAGTTCCT
NT005	PDS genomic DNA	GCTTCGCAAGTAGCAGCATC
NT008	PDS genomic DNA	GGTGCAGGCAATGTTTCAGG
Tia_PDS_sgRNA1_NGS	sgRNA1 target (F)	GGGGAAATGCCTTGAACAG
Tia_PDS_sgRNA1_NGS	sgRNA1 target (R)	TTCATACTCCCGCATGGC
Tia_PDS_sgRNA2_NGS	sgRNA2 target (F)	TCGTGATTGCTGGAGCAGG
Tia_PDS_sgRNA2_NGS	sgRNA2 target (R)	CCTTTCCACCCAAAACATCCC